JOURNAL OF AGRICULTURAL AND FOOD CHEMISTRY

Article

pubs.acs.org/JAFC

Comprehensive MS and Solid-State NMR Metabolomic Profiling Reveals Molecular Variations in Native Periderms from Four *Solanum tuberosum* Potato Cultivars

Wenlin Huang,[†] Olga Serra,[‡] Keyvan Dastmalchi,[†] Liqing Jin,[†] Lijia Yang,[†] and Ruth E. Stark*[,†]

[†]Department of Chemistry and Biochemistry, The City College of New York, City University of New York Ph.D. Programs in Chemistry and Biochemistry, and CUNY Institute for Macromolecular Assemblies, New York, New York 10031, United States

[‡]Laboratori del Suro, Departament de Biologia, University of Girona, Campus Montilivi s/n, Girona, E-17071 Spain

Supporting Information

ABSTRACT: The potato (*Solanum tuberosum* L.) ranks third in worldwide consumption among food crops. Whereas disposal of potato peels poses significant challenges for the food industry, secondary metabolites in these tissues are also bioactive and essential to crop development. The diverse primary and secondary metabolites reported in whole tubers and wound-healing tissues prompted a comprehensive profiling study of native periderms from four cultivars with distinctive skin morphologies and commercial food uses. Polar and nonpolar soluble metabolites were extracted concurrently, analyzed chromatographically, and characterized with mass spectrometry; the corresponding solid interfacial polymeric residue was examined by solid-state ^{13}C NMR. In total, 112 secondary metabolites were found in the phellem tissues; multivariate analysis identified 10 polar and 30 nonpolar potential biomarkers that distinguish a single cultivar among Norkotah Russet, Atlantic, Chipeta, and Yukon Gold cultivars which have contrasting russeting features. Compositional trends are interpreted in the context of periderm protective function.

KEYWORDS: *Solanum tuberosum L., metabolomics, LC-MS, TOF-MS, suberin, potato skin*

INTRODUCTION

The potato skin plays significant roles in both agricultural practice and food production. The botanical term for potato skin is phellem, which, together with the meristematic mother layer phellogen and the parenchymatic phelloderm, forms the periderm. The periderm protects the tubers from microbial invasion, water loss, and UV radiation.[1,2] These beneficial functions, which are essential to achieve robust crop yields and maintain the marketability of food products, are attributed to the suberin polymer and associated waxes that together form a cell-wall composite. The potato skin is also a major waste product and thus a potential liability in the food industry.[3] At the same time, this plant tissue can be a potentially useful commodity for food, drug, cosmetic, and medical applications because it contains bioactive metabolites including phenolic, fatty acid, and glycoalkaloid compounds.[4−6]

To characterize the insoluble polymeric constituents of the periderm, chemical breakdown of aliphatic suberin to release and identify soluble monomers has been achieved in external tree bark (cork) and in native and wound-healing periderms of potato tubers.[7−9] Using potato periderms, for instance, depolymerization of the biopolymer by transesterification revealed a variety of aliphatic monomeric constituents: primarily long-chain α,ω-dicarboxylic acids and ω-hydroxyfatty acids with different degrees of unsaturation as well as $C_{16}-C_{30}$ long-chain fatty acids and fatty alcohols.[7,10] This compositional information has been augmented more recently by isolation of oligomeric fragments that are thought to link suberin's aliphatic and aromatic molecular domains.[11−13] In a complementary fashion, thioacidolysis of ether linkages has helped to define the polyphenolic structures as lignin-like guaiacyl and syringyl moieties linked to amides.[14−16] A semiquantitative analysis accounting for these chemical degradation products, when coordinated with ultrastructural examination of the suberized tissues, has led to several conceptual models for the macromolecular architecture of the chemical building blocks.[9,17]

Conversely, the intact suberized potato cell walls have been characterized directly, using solid-state ^{13}C nuclear magnetic resonance (NMR) and Fourier transform infrared spectroscopy (FT-IR) to identify the major polyaliphatic, polyphenolic, and alkoxy functional groups; with NMR also providing estimates of their proportions and assessments of their respective molecular flexibilities.[18−24] Notwithstanding the valuable structural information that has emerged from the various studies, neither partial degradation to obtain small molecular fragments nor specification of chemical moieties in the intact materials has provided a complete picture of this essential protective macromolecular composite.

In addition to the insoluble protective suberin polymer, potato tubers accumulate a variety of secondary metabolites, including phenolics, polyamines, flavonoids, and glycoalkaloids which defend the plant against microbial pathogens.[25−27] These small molecules can be biosynthetic intermediates of the polyesters, developmental modulators, or defensive agents in

Received: November 17, 2016
Revised: February 12, 2017
Accepted: February 18, 2017
Published: February 18, 2017

DOI: 10.1021/acs.jafc.6b05179
J. Agric. Food Chem. 2017, 65, 2258−2274

their own right.[2] To identify the soluble metabolites embedded within suberized potato tissues, solvent extraction followed by analyses performed by either gas or liquid chromatography combined with mass spectrometry (GC-MS and LC-MS, respectively) are typically used for profiling. For native potato tubers and periderms, several efficient extraction protocols have been introduced for metabolites with a range of polarities.[28−30] These methods have yielded a range of nonpolar waxes in addition to the polyphenolics, polyamines, flavonoids, and glycoalkaloids described above. Differences in polar metabolite content have been demonstrated for whole tubers with varying genotypes and presumed pathogen resistance,[31−34] but statistical comparisons among the periderm metabolite pools in these plants have so far been limited to wound-healing tissues.[35−37]

In native potato tuber periderms, aliphatic products derived from transesterification of suberized tissues have been found to be altered upon down-regulation of suberin-related genes by RNA interference.[12,38−42] Moreover, solid-state ^{13}C NMR of the corresponding suberin-enriched cell walls showed significant differences in the prevalence of aliphatic vs aromatic moieties and in chemical recalcitrance of periderms for which a feruloyl transferase enzyme was silenced, suggesting distinctive structures for their respective suberin biopolymers.[24] Despite these significant advances in the molecular characterization of potato tubers, it is desirable to adopt a metabolomics approach that combines powerful analytical measurements (*e.g.,* MS or NMR) with multivariate statistical data analysis to critically evaluate changes in the metabolite pool deriving from physiological stimuli or genetic modification.

Russeting of potato periderms, a rough skin texture described as a consequence of rapid tuber expansion that leads to cracking, is sometimes valued in baking potatoes but can diminish crop yields by permitting tuber desiccation.[43] Recently, we used developing potato wound periderms to demonstrate the feasibility of identifying potential biomarkers that discriminate among four cultivars with differing breeding history, maturation, food uses, and skin russeting character (cv. Norkotah **R**usset, **A**tlantic, **C**hipeta, and **Y**ukon Gold, collectively referred to as **RACY**; Table 1) and according to the choice of time point after wounding.[36,37] In these prior studies, we extracted both polar and nonpolar metabolite mixtures simultaneously with a solid suspension that contains the suberin biopolymers; we used LC-MS, GC-MS, and ^{1}H NMR for metabolomic analyses, solid-state ^{13}C NMR to determine proportions of the major functional groups, and radical scavenging assays to assess the stress-induced antioxidant capability of the soluble extracts.

Table 1. Characteristics of Profiled Potato Cultivars[a]

Cultivar	Genetic Origin	Skin type	Maturation	Cooking type
Atlantic	Wauseon × USDA B5141-6 (Lenape)	White-round	Midseason	Chipped
Chipeta	USDA WNC612-13 × USDA Wischip	White-round	Late	Chip stock
Norkotah	ND9526-4 Russ × ND9687-5 Russ	Russet	Early-Medium	Baking
Yukon Gold	W5279-4 × Norgleam	White-round	Medium-Early	Baking, Boiling, French-fried

[a]http://potatoassociation.org/

The current complementary work compares native periderms of these four potato cultivars using principal component analysis (PCA) and hierarchical cluster analysis (HCA), and then it identifies marker metabolites that contribute significantly to their compositional distinctions through orthogonal partial least-squares discriminate analysis (OPLS-DA). Moreover, we present a more complete accounting of the soluble metabolite profiles and coordinate the structural information from the polar, nonpolar, and solid polymeric materials. Distinctive chemical compositions are identified for native vs wound periderms and interpreted in the context of suberin biosynthesis. These evaluations for native periderms provide molecular insights into russeting and can inspire the development of potato cultivars exhibiting robust resistance to crop loss threats from desiccation, infection, and wound-related spoilage.

MATERIALS AND MEHTHODS

Plant Material. Freshly harvested potato tubers from Norkotah Russet, Atlantic, Chipeta, and Yukon Gold cultivars grown during the 2011 season were shipped overnight from the Agriculture and Natural Resources Division, University of California at Davis. The samples were washed with deionized water, and the skin was peeled using a flat spatula and avoiding contamination from the inner parenchymatic tissue before they could develop resistance to excoriation,[44] and frozen immediately in liquid nitrogen. The frozen potato periderms were ground to powder with a precooled mortar and pestle, and then they were lyophilized to dryness prior to storage at −70 °C in vacuum-sealed bags.

Chemicals. Methanol (HPLC grade) and chloroform (analytical grade) were purchased from Fisher Scientific (Pittsburgh, PA). Water was obtained using a Milli-Q purification system (Millipore, Billerica, MA). HPLC/MS grade water and acetonitrile (ACN) were purchased from J. T. Baker (Phillipsburg, NJ). Formic acid (puriss. p.a. for mass spectroscopy) was from Fluka Chemie/Sigma-Aldrich (St. Louis, MO). Anhydrous pyridine (analytical grade) was purchased from Sigma-Aldrich. *N*-Methyl-*N*-(trimethylsilyl) trifluoroacetamide (MSTFA) was supplied by Thermo Scientific (Bellefonte, PA). The C7−C40 saturated alkane standards were obtained from Supelco (Bellefonte, PA).

Extraction and Derivatization Procedures. Soluble metabolites were extracted from the native periderms according to established methods.[30] Seven 5-mg freeze-dried replicate periderm samples from each of the four potato cultivars were each added to a solution of 1.54 mL of methanol and 0.33 mL of deionized water and vortexed for 60 s. An additional 0.77 mL of chloroform was added to the mixture, which was vortexed for another 60 s. After shaking in a benchtop incubator at 400 rpm for 15 min, the resulting sample contained a biphasic solution with a suspended solid. Additional 0.77 mL portions of chloroform and deionized water were added to the sample solution, which was then vortexed for 60 s and ultrasonicated for 15 min. Centrifugation at 3000 rpm for 15 min at 4 °C produced a two-phase solution comprised of an upper methanol−water phase (containing polar metabolites) and a lower chloroform phase (containing nonpolar metabolites), which were separated by an interfacial layer containing solid particulates (polymers).

The polar extract in the upper layer was removed with a glass Pasteur pipet, transferred to a glass vial, dried under nitrogen gas, and reconstituted in a 98:2 (v/v) water−acetonitrile mixture containing 0.1% formic acid for LC-MS analysis; seven replicates per cultivar were analyzed. The nonpolar extract of the lower layer was also transferred to a glass vial with a Pasteur pipet and dried for GC-MS analysis. Each dried nonpolar extract was reconstituted in 50 μL of anhydrous pyridine and derivatized with 80 μL of MSTFA + 1% trimethylchlorosilane, and then silylated by shaking at 50 °C for 1 h; six replicates per cultivar were analyzed because a few of the samples were lost during processing. The trimethylsilylated samples were equilibrated at room temperature before GC-MS injection. The interfacial

DOI: 10.1021/acs.jafc.6b05179
J. Agric. Food Chem. 2017, 65, 2258−2274

solids were filtered and washed with distilled water, and then treated successively with *Aspergillus niger* cellulase (MP Biomedicals, Illkirch, France) and pectinase (Sigma-Aldrich) to remove unsuberized cell-wall materials as described previously.[24,37,45] Waxes and soluble lipids were removed by Soxhlet extraction under reflux conditions, using methanol, chloroform, and hexane successively for 48 h each. The suberin-enriched periderm samples were dried and used for ^{13}C NMR experiments as described below.

Liquid Chromatography—Electrospray Ionization Mass Spectrometry (LC-ESI-MS). The LC-ESI-MS system consisted of a Shimadzu LC-20 AD HPLC chromatograph (Canby, OR) and an Applied Biosystems 4000 Q Trap mass spectrometer (Foster City, CA, USA). A 150 × 4.6 mm i.d., 3.0 μm, Ascentis C18 reverse-phase column (Supelco Corp., Bellefonte, PA) was used with a flow rate of 0.5 mL/min and an injection volume of 10 μL. The column oven temperature was set to 30 °C. A gradient was programmed for a mobile phase mixture of 0.1% formic acid in water (A) and 0.1% formic acid in acetonitrile (B), varying linearly from 2 to 35% B (v/v) for 35 min, from 35 to 98% B until 45 min, and holding at 98% until 51 min. An equilibration time of 10 min was allowed between samples, which were held at the initial mobile phase composition (2% B).

MS spectra were obtained in both negative and positive ion electrospray (ESI) modes and processed using Analyst 1.4.2 software. The ESI probe was operated at −4.5 kV (negative) or 5.0 kV (positive), using a cone voltage of 25 V. The source and desolvation temperatures were 120 and 350 °C, respectively. The nitrogen nebulizing and drying gas pressures were set to 50 and 40 psi, respectively. Each spectrum was recorded between *m*/*z* 100 and 1300 in centroid mode with a duration of 2s/scan and an interscan time of 0.1 s.

Tandem mass spectrometric analyses (LC-ESI-MS/MS) were conducted using information-dependent acquisition (IDA) in Analyst 1.4.2. An IDA method was programmed to combine Enhanced MS (EMS) as the survey scan and enhanced product ion (EPI) as the dependent scan in the same injection. Five of the most intense peaks in the EMS scan were selected for the EPI scan. EPI scans at five different collision energies (−35, −50, −65, −80, and −95 eV) were monitored to obtain an optimum fragment pattern. The declustering potential was set to −140 V, and the collision energy spread was 10 eV. Chlorogenic acid and rutin, two compounds found commonly in potato tubers,[33,34,46] were used as reference standards.

Time of Flight-Mass Spectrometry (TOF-MS). Metabolite separation was performed under the same conditions as the LC-ESI-MS experiments, using an Agilent 1200 HPLC system with a quaternary pump, column heater, DAD detector, and fraction collector (Santa Clara, CA). The fractions were injected at a flow rate of 10 μL/min using a Harvard syringe pump and collected every half minute to obtain high-resolution masses of metabolites with a Waters LCT premier XE mass spectrometer (Milford, MA, USA) in negative electrospray ionization mode with >10,000 resolution. The desolvation gas flow was set to 800 L/h at a temperature of 350 °C, and the cone gas flow was set to 10 L/h. The source temperature was set to 120 °C. The capillary voltage was set to −3.0 kV, and the cone voltage was set to 40 V. The data acquisition rate was 0.15 s/scan, with a 0.01 s interscan delay using dynamic range enhancement for 1 min. To ensure mass accuracy, a reference solution of leucine−enkephalin (Sigma-Aldrich, *m*/*z* 556.2771) was introduced continuously using the LockSpray interface. The flow rate of the reference solution was 100 μL/min, and the concentration was 400 ng/mL. All data were collected from *m*/*z* 100 to 1300 in centroid mode. The possible elemental compositions for each accurate mass were calculated using a monoisotopic mass type with Masslynx 4.1 software.

Gas Chromatography-Mass Spectrometry (GC-MS). GC-MS analysis was performed using a QP2010 plus instrument (Shimadzu USA, Canby, RI) equipped with an AOC-5000 automatic injection system. A RESTEK (Bellefonte, PA) Rtx-5MS column (30 m × 0.25 mm i.d., film thickness 0.25 μm) was used with a temperature program following Yang and Bernards:[35] an initial setting of 70 °C for 5 min, followed by an increase of 5 °C per min to 310 °C, and finally a hold of 11 min for a total run time of 64 min. The injection temperature was kept at 250 °C; helium was used as a carrier gas with a constant flow rate of 1 mL/min. A 1.0-μL sample was injected using the splitless mode. The mass spectrometer was tuned and calibrated before data acquisition using the AutoTune function to optimize system performance and consistency. MS operating conditions were as follows: ionization voltage: 70 eV; ion source temperature: 200 °C; interface temperature: 280 °C; full scan mode in the *m*/*z* range 40−600 with a scan time of 0.50 s.

All GC-MS chromatograms were acquired starting with a retention time of 8 min to exclude solvent surge. The sequence of data acquisition was cycled among the cultivars to minimize the effects of any time-dependent retention time variations during data collection. Three blank samples subjected to the identical protocols were also analyzed at the beginning, middle, and end of the experimental sequence to detect any possible contamination (*e.g.*, from sample preparation or instrumentation, solvent or reagent impurities) and to monitor the instrument performance (baseline consistency and carryover).

Compound identification was accomplished by using a combination of retention time and retention index values using Shimadzu GCMSsolution version 2.53 software and by reference to a set of C7−C40 alkane standards. Retention time corrections were performed on the basis of the observed retention times of the standard alkane mixtures by using the automatic Adjustment of Retention Time function of the Shimadzu software. Mass searches were conducted by using the integrated libraries of the National Institute of Standards and Technology (NIST 08, Gaithersburg, MD) and Wiley Registry 9 (2008). Spectral peaks were identified as compounds from the libraries if they possessed a similarity index of more than 80%, whereas those with smaller similarity indices were designated as unknown molecules. Given the similar MS patterns of the *n*-alkane fragments, identification of the *n*-alkanes was confirmed by their retention indices.

Solid-State NMR Analysis. Identification and quantitation of the major molecular groupings in the suberin-enriched periderms used data from magic-angle spinning ^{13}C NMR spectra acquired with cross- and direct-polarization from ^{1}H nuclei, respectively (CPMAS and DPMAS) on 3−6 mg powdered samples. For these experiments, we used a four-channel Varian (Agilent) DirectDrive I (VNMRS) NMR spectrometer operating at a ^{13}C frequency of 150.757400 MHz and equipped with a 1.6 mm HXY FastMAS probe spinning at 10.00 ± 0.02 kHz (Varian Instruments, Palo Alto, CA, USA). Typical instrumental parameters included a CP contact time of 1.5 ms, a 200 kHz ^{1}H heteronuclear decoupling strength achieved using the SPINAL method,[47] an acquisition time of 25 ms, and a delay time of 3 s between 9000 successive acquisitions. For DPMAS experiments, a delay time of 100 s was used between each of 3000 spectral acquisitions. (Efficient multiCPMAS methods for quantitation[48] were subsequently implemented for wound potato periderm materials,[37] but cross-polarization was compromised for highly mobile moieties present in the native periderms.)

The resulting spectra were processed using ACD/NMR Processor Academic Edition (version 12; Advanced Chemistry Development, Inc., Toronto, ON, Canada) and/or Varian VNMRJ (version 2.2c) software. Chemical shift values were referenced to the methylene resonance of an external adamantane sample (Sigma-Aldrich) set to 38.48 ppm.[49] Integrated peak intensities were measured from the DPMAS spectra to estimate the relative numbers of carbonyl groups (carboxyls and/or amides, 160−180 ppm), multiply bonded aromatics and alkenes (110−160 ppm), oxygenated aliphatics (CH_nO, 46−110 ppm), and long-chain methylene groups ($(CH_2)_n$, 10−46 ppm). Three independent methods were used: (a) counting pixels with Photoshop software using identical chemical shift limits for the four potato cultivars; (b) counting pixels using shift limits adjusted to best represent the peaks observed in each spectrum; and (c) cutting and weighing the peaks in each hard-copy spectrum following the guidelines of method (b).[24,37,50] The resulting functional group ratios were consistent within 5−15%.

Processing of LC-MS and GC-MS Data. To obtain files that can be recognized by most mass spectrometry software using ProteoWizard 3.0 (http://proteowizard.sourceforge.net/), the packed LC-MS

DOI: 10.1021/acs.jafc.6b05179
J. Agric. Food Chem. 2017, 65, 2258−2274

raw data (extension *.wiff) from Analyst 1.4.2 were unzipped and converted to mzXML files; the GC-MS chromatograms were converted into ANDI files (Analytical Data Interchange Protocol, *.cdf) using GCMSsolution software. All potato MS chromatograms were then imported and processed using MZmine version 2.4, an open source LC/GC-MS data processing package (http://mzmine.sourceforge.net/) for metabolomics analysis.[51,52] A typical workflow for MZmine processing of mass spectral data consisted of raw data import, generation of mass lists for each scan using Mass Detector, detection of chromatograms using Chromatogram Builder, deconvolution of chromatograms into individual peaks, alignment using the Join Aligner, and gap filling using Peak Finder.

For LC-MS data, a corrected range of retention times (0−45 min) and baseline intensities (>2 × 10^5) was employed to remove peak noise and unreliable features in the elevated baseline region (45−51 min). Parameters for Min time span, Min peak duration, m/z tolerance, and retention time tolerance were adjusted to 0.1, 0.1, 0.2 and 0.3, respectively, to optimize the separation between cultivars by principal component analysis. For GC-MS, a corrected range of retention times (17−55 min) and baseline intensities (>7 × 10^2) was employed to remove peak noise and fragment peaks attributable to derivatization agents. The parameters of Min time span, Min peak duration, m/z tolerance, and retention time tolerance were optimized to 0.1, 0.1, 0.3 and 0.1, respectively, to achieve the clearest separation between cultivars in the principal component analysis. For both sets of data, the aligned peak lists with area integration were exported to *.csv files and normalized to the total peak area using Microsoft EXCEL to remove any systematic bias. To compare the amounts of soluble nonpolar aliphatic constituents in the four potato cultivars, the area of each peak in the total ion chromatogram was integrated and normalized to the total area.

Multivariate Statistical Analysis. The aligned and normalized LC-MS and GC-MS data sets were imported into the SIMCA-P+13 software package (Umetrics, Umea, Sweden) for statistical data analysis. For this purpose, all variables were Pareto-scaled, so as to increase the importance of low-abundance ions and minimize the influence of noise and artifacts.[53] To discriminate between potato cultivars, principal component analysis (PCA) was carried out. This unsupervised method for pattern recognition analysis, conducted without *a priori* knowledge of the data set, was conducted initially to identify intrinsic variations and any obvious outliers within each data set, yielding an overview of metabolite variation among the potato cultivars. The projections of each variable on the first, and subsequently the second and third principal components, reduce the dimensionality of multivariate data but preserve most variances within it.

Two-dimensional PCA score plots were used to determine whether the overall metabolite compositions could be distinguished as a function of cultivar. Then, hierarchical cluster analysis (HCA) served to group the relatively similar samples based on their measured ions in LC-MS or GC-MS experiments. To determine the metabolites responsible for differences among potato cultivars, orthogonal partial least-squares discriminate analysis (OPLS-DA) was used to generate scatter plots (S-plots) from which potential markers were chosen and identified according to retention time and m/z value, based on the magnitude of the variation in abundance (p[1]) and the reliability of the effect (p(corr)[1]) within the data set. Variable line plots were used to verify whether the potential markers were specific to a particular cultivar. The metabolites were identified by comparison of the MS data with published results or reference databases, as described below for the specific LC-MS and GC-MS experiments.

RESULTS AND DISCUSSION

Design of the Periderm Extraction Protocol. The overall quality of a metabolomic analysis can be compromised by incomplete extraction; it is thus essential to select solvent(s) that extract the largest range and quantity of metabolites while remaining nondestructive.[54] However, no single solvent can extract all metabolites from a typical plant tissue. In the current study, the metabolites within native periderms of four potato cultivars were extracted with a methanol−water−chloroform (4:2:4 v/v/v) mixture.[30] This two-phase system simultaneously extracts not only polar hydrophilic metabolites but also nonpolar hydrophobic compounds. To maximize the completeness of metabolite recovery from the potato periderm tissues, sequential steps were employed, including an initial hydrophilic extraction (typically with CH_3OH−H_2O) followed by vortexing, ultrasonication, and then hydrophobic extraction (typically with $CHCl_3$). For hydrophilic extraction, a mixture of methanol and water is the most popular combination for metabolomics studies because of its proven ability to extract a wide range of metabolites, e.g., amino acids, organic acids, sugars, alkaloids, and phenolic acids,[55] although the overall recovery of extracts by this solvent mixture is slightly lower than that of pure CH_3OH.[56] For hydrophobic extraction, a CH_3OH−$CHCl_3$−H_2O system yields high response ratios for fatty acids such as hexadecanoic acid (C16) and octadecanoic acid (C18).[56] Sonication also provides an efficient method to disrupt the potato cells and thus reduce extraction time. Moreover, the advantages of the current CH_3OH−H_2O−$CHCl_3$ extraction include the compatibility of most organic solvents with diverse analytical platforms such as GC-MS, LC-MS, and NMR spectroscopy, the absence of salt precipitates, and the relative ease of solvent evaporation. Finally, this two-phase extraction produces two easily separated layers and an interfacial solid suspension, allowing for comprehensive "holistic" structural profiling of soluble metabolites with a range of polarities in conjunction with solid polymeric materials that comprise the native potato periderm.

Profiling and Identification of Polar Metabolites. Reverse phase LC-MS profiling of aqueous-methanol periderm extracts revealed 37 major MS peaks from each of the four potato cultivars. Seven periderm replicates from different potato tubers of each cultivar type were analyzed using identical LC-MS parameters. Representative chromatograms from the four cultivars are plotted in Figure 1. Although a largely similar set of ions was detected in all potato samples,

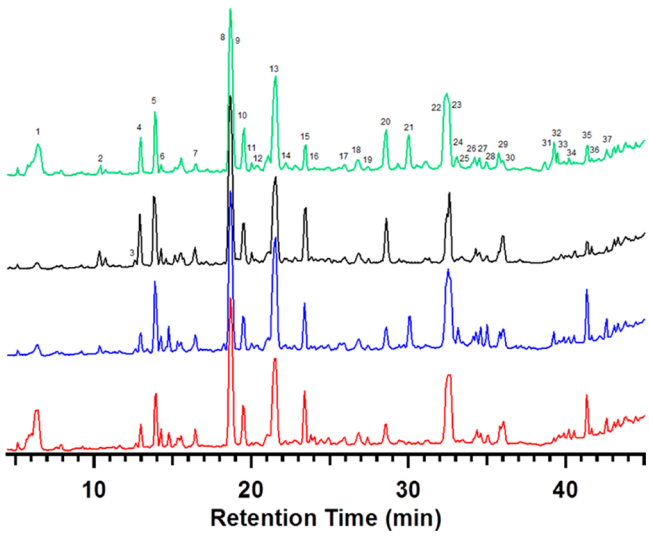

Figure 1. LC-MS data for polar extracts from native potato periderms, showing representative total ion current chromatograms in negative mode for each of the four cultivars. The traces are color coded for Yukon Gold (green), Norkotah Russet (black), Chipeta (blue), and Atlantic (red).

DOI: 10.1021/acs.jafc.6b05179
J. Agric. Food Chem. 2017, 65, 2258−2274

distinctions among the studied cultivars were evident from significant and reproducible differences in their relative intensities.

Molecular elucidation of metabolites is achieved most definitively using a reference standard. Because standard compounds are generally unavailable for potato periderm extracts, the structural identifications reported herein were made provisionally using the retention time, MS/MS fragmentation pattern, and accurate mass obtained in TOF experiments and additionally by comparison to prior published data for similar plant species. Two steps were typically employed for metabolite characterization. First, the optimum MS/MS fragmentation pattern of the polar metabolite was obtained by tandem mass spectrometry, optimized using five different collision energies in negative mode. Second, the possible molecular formula was determined by monoisotope calculation from the high-accuracy mass measured in TOF-MS experiments. The molecular structure could then be confirmed through a SciFinder search if the observed metabolite had been reported in potatoes and/or related plants and provided that the characteristic MS/MS ions matched our observations.

A total of 27 of the 36 analyzed potato metabolites in the aqueous−methanol extracts were identified by these procedures; the compound class was deduced for an additional four unidentified compounds, based on their polarities and fragmentation patterns. Table 2 lists five classes of polar secondary metabolites in native periderms of potato cultivars: phenolic amines, phenolic acids, a flavonoid, glycoalkaloids, and saponins. These classes of metabolites, including one (saponins) that has not been reported previously in the native periderm of potato tubers, provide a comprehensive metabolic profile that complements our prior report of potential polar biomarkers in potato wound periderms from the same cultivars.[36]

Phenolic amines, in particular polyamines, are important compounds involved in plant growth, development, and stress responses.[57−59] They occur primarily as putrescines, spermines, and spermidines, in which hydroxycinnamic acid derivatives are bound to aliphatic amine groups. Eleven polyamines were identified by their exact masses and MS/MS fragmentation patterns, including three putrescine derivatives (peaks ***2***, ***4***, and ***7*** listed in Table 2), five spermine derivatives (***5***, ***6***, ***15***, ***16***, and ***24***) and three spermidine derivatives (***9***, ***11***, and ***21***), with molecular structures shown in Figure 2a.

N-Caffeoylputrescine (peak ***4***) and *N*-feruloylputrescine (peak ***7***) have been identified previously in potato periderms.[31,32,34,60] Compound ***2*** eluted before *N*-caffeoylputrescine (***4***) and displayed related MS characteristics: *m*/*z* of 251 compared with 249 and a characteristic fragment ion at *m*/*z* 137 compared with 135, suggesting identification as *N*-dihydrocaffeoyl putrescine (***2***) and a dihydrocaffeoyl fragment ion, respectively.

Compounds ***5***, ***15***, and ***24*** displayed $[M-H]^-$ ions at *m*/*z* of 529, 693, and 857, respectively. The three negative ions exhibited *m*/*z* differences corresponding to neutral losses of 164 (a dihydrocaffeoyl moiety), representing spermines with bis-, tris-, and tetra-dihydrocaffeoyl substituents, respectively, on their amine groups. Their common characteristic fragment ions (MS/MS) were observed at *m*/*z* 285, 365, and 407, supporting their structural similarities. By reference to prior reports,[28] it was possible to identify these compounds as N^1,N^{12}-bis(dihydrocaffeoyl) spermine (***5***), N^1,N^4,N^{12}-tris(dihydrocaffeoyl) spermine (***15***), and N^1,N^4,N^9,N^{12}-tetra(dihydrocaffeoyl) spermine (***24***).

Compound ***6*** eluted after ***5*** (N^1,N^{12}-dihydrocaffeoyl spermine) and displayed related MS ions: an $[M-H]^-$ ion at *m*/*z* 527 compared with 529, and MS/MS fragments at *m*/*z* 363 and 405 compared with *m*/*z* 365 and 407. Thus, one of the dihydrocaffeoyl substituents was evidently dehydrogenated to a caffeoyl group and ***6*** could be tentatively assigned as N^1,N^{12}-bis(caffeoyl, dihydrocaffeoyl) spermine. Analogously to the case of ***6***, compound ***16*** displayed a $[M-H]^-$ ion at *m*/*z* 691 and eluted after N^1,N^4,N^{12}-tris(dihydrocaffeoyl) spermine (***15***, *m*/*z* 693). MS/MS spectra showed that ***15*** and ***16*** shared similar fragments including *m*/*z* 529, 407, and 365, suggesting closely related structures for these two compounds. However, the observation of a fragment ion *m*/*z* 161 for ***16***, compared with *m*/*z* 163 for ***15***, indicated that a caffeoyl group rather than the dihydrocaffeoyl moiety was attached to an amine group. Therefore, we identified ***16*** as tris(N^1-caffeoyl, N^4,N^{12}-dihydrocaffeoyl) spermine.

Compounds ***9*** and ***21*** were characterized as two spermidines with *m*/*z* 472 and 636, respectively, in negative mode, corresponding to N^1,N^8-bis(dihydrocaffeoyl) spermidine and N^1,N^4,N^8-tris(dihydrocaffeoyl) spermidine.[28] These two compounds were confirmed by common characteristic MS/MS fragments at *m*/*z* 186, 228, 308, 350, and 472, along with high accuracy masses from TOF experiments. Compound ***11***, which displayed $[M-H]^-$ at *m*/*z* 470, was found to share characteristic MS/MS ions with ***9*** and ***21*** at *m*/*z* 186 and 308, suggesting a spermidine structure. Similarly to ***16***, ***11*** gave a fragment ion at *m*/*z* 161, indicating a caffeoyl group. As a result, ***11*** was tentatively identified as bis(N^1-caffeoyl, N^8-dihydrocaffeoyl) spermidine.

Three major compounds (***8***, ***10***, ***13***) displayed the same $[M-H]^-$ ions at *m*/*z* 353 in negative mode LC-MS/MS experiments. The three compounds were well separated under our LC experimental conditions, eluting at 18.7, 19.5, and 21.5 min, respectively. They were identified as isomeric chlorogenic acids: chlorogenic acid (3-*O*-caffeoylquinic acid) (***8***), neochlorogenic acid (5-*O*-caffeoylquinic acid) (***10***), and cryptochlorogenic acid (4-*O*-caffeoylquinic acid) (***13***), respectively.[61] The observed MS/MS fragment patterns with base peaks at *m*/*z* 191 ([quinic acid−H]$^-$), and 173 ([quinic acid−H−H_2O]$^-$) corresponded to the 3-*O*, 5-*O*, and 4-*O* isomers reported previously.[28,62]

Compounds **22** and **23**, which eluted at 32.4 and 32.6 min, respectively, were identified as α-chaconine and α-solanine, the two principal glycoalkaloids reported in potatoes. Both compounds displayed adduct ions $[M-HCOO]^-$ in negative-mode MS. These two glycoalkaloids have the same aglycone but are attached to different sugar moieties: α-chaconine has two rhamnoses and one glucose, whereas α-solanine has one rhamnose, one glucose, and one galactose.[63] Characteristic MS/MS fragment ions of α-chaconine were observed at *m*/*z* 850 $[M-HCOO]^-$, 704 $[M-HCOO-146]^-$, and 558 $[M-HCOO-146-146]^-$, where the neutral loss of 146 corresponds to a rhamnose. An $[M-H]^-$ ion at *m*/*z* 936 was detected for compound ***26***, which showed fragment ions at *m*/*z* 850 and 704 matching the characteristic MS/MS ions of ***22***, and thus suggested that ***26*** possesses an α-chaconine residue. Further structural elucidation of the latter compound should be possible after purification and spectroscopic characterization by NMR methods.

DOI: 10.1021/acs.jafc.6b05179
J. Agric. Food Chem. 2017, 65, 2258−2274

Table 2. Metabolites Isolated from Polar Extracts of Four Potato Cultivars

No.	RT[a] (min)	Compound Name	Structural Class[b]	$[M-H]^-/[M+H]^+$	MS/MS ($[M-H]^-$)	Exact Mass	Calcd Mass	Error (ppm)	Lit. ref
1	6.4	Quinic acid, $C_7H_{12}O_6$	quinic acid	191/193	85(21), 87(20), 111(100), 129(4), 191(9)	191.0557	191.0561	−2.1	79
2	10.4	*N*-dihydrocaffeoylputrescine, $C_{13}H_{20}N_2O_3$	phenolic amine	251/253	93(47), 109(13), 121(100), 129(47), 137(7), 251(3)	251.1399	251.1401	−0.8	this work
3	12.6	Unknown		409/−	97(20), 139(4), 167(4), 223(3), 241(100), 409(83)				
4	13.0	*N*-Caffeoylputrescine, $C_{13}H_{18}N_2O_3$	phenolic amine	249/251	89(4), 107(6), 134(25), 135(100), 147(10), 148(11), 161(14), 176(11), 190(9), 207(8), 249(5)	249.1234	249.1244	−4.0	28
5	13.9	N^1,N^{12}-bis(dihydrocaffeoyl) spermine, $C_{28}H_{42}N_4O_6$	phenolic amine	529/531	93(8), 109(13), 115(30), 121(60), 163(9), 228(6), 243(44), 285(15), 363(10), 365(10), 407(84), 419(10), 529(53)	529.3057	529.3031	4.9	28
6	14.3	*N*-(caffeoyl, dihydrocaffeoyl) spermine, $C_{28}H_{40}N_4O_6$	phenolic amine	527/529	161(62), 243(8), 363(10), 365(100), 405(5), 527(34)	527.2877	527.2875	0.4	80
7	16.4	*N*-feruloylputrescine, $C_{14}H_{20}N_2O_3$	phenolic amine	263/265	133(4), 161(18), 176(6), 190(8), 204(13), 247(100), 248(82), 263(23)	263.1381	263.1396	−5.7	31,60
8	18.7	3-*O*-caffeoyl quinic acid (chlorogenic acid), $C_{16}H_{18}O_9$	phenolic acid	353/355	191(100), 353	353.0863	353.0873	−2.8	61
		Dimer, $C_{32}H_{36}O_{18}$		707/709	173(73), 179(7), 341(20), 353(26), 371(23), 527(10), 545(100), 707(40)	707.1843	707.1823	2.8	
9	18.7	N^1,N^8-bis(dihydrocaffeoyl) spermidine, $C_{25}H_{35}N_3O_6$	phenolic amine	472/474	93(9), 121(24), 186(27), 228(9), 308(100), 350(18), 472(5)	472.2439	472.2448	−1.9	28
10	19.5	5-*O*-caffeoyl quinic acid (neochlorogenic acid), $C_{16}H_{18}O_9$	phenolic acid	353/355	135(20), 179(32), 191(100), 353(6)	353.0877	353.0873	1.1	61
11	20.0	bis(N^1-caffeoyl, N^8-dihydrocaffeoyl) spermidine, $C_{25}H_{33}N_3O_6$	phenolic amine	470/472	135(100), 161(12),186(1), 291(51), 308(24), 334(66), 348(2), 470(5)	470.2269	470.2291	−4.7	80
12	20.4	Caffeic acid derivatives, $C_{21}H_{16}O_{11}$	phenolic acid	443/−	150(18), 165(35), 167(17), 195(9), 245(36), 275(17), 315(6), 363(2), 443(100)	443.0619			
13	21.5	4-*O*-caffeoyl quinic acid (cryptochlorogenic acid), $C_{16}H_{18}O_9$	phenolic acid	353/355	135(33), 173(100), 179(76), 191(49), 353	353.0854	353.0873	−5.4	61
14	22.2	Unknown		705/−	191(4), 339(14), 513(100), 548(3), 705(15)	705.1668	705.1667	0.1	
15	23.4	N^1,N^4,N^{12}-tris(dihydrocaffeoyl) spermine, $C_{37}H_{50}N_4O_9$	phenolic amine	693/695	109(16), 115(18), 121(39), 163(11), 243(46), 244(7), 285(53), 365(86), 366(12), 407(100), 419(12), 449(35), 529(78), 553(6), 571(42), 583(6), 693(19)	693.3481	693.3505	−4.8	28
16	23.8	Tris(N^1-caffeoyl,N^4,N^{12}-dihydrocaffeoyl) spermine $C_{37}H_{48}N_4O_9$	phenolic amine	691/693	135(24), 161(29), 269(12), 348(8), 365(30), 391(38), 407(23), 433(27), 529(100), 555(72), 691(8)	691.3324	691.3343	−2.7	this work
17	25.8	Rutin, quercetin-3-*O*-rutinoside, $C_{27}H_{30}O_{16}$	Flavonoid	609/−	179(8), 255(5), 271(18), 300(100), 301(45), 609(26)	609.1446	609.1456	−1.6	28
18	26.8	Unknown		531/−	147(5), 159(5), 191(19), 229(25), 267(6), 269(9), 295(19), 313(5), 339(100), 531(37)	531.1128	531.1138	−2.0	
19	27.5	Caffeic acid derivative, $C_{35}H_{34}O_8$	phenolic acid	581/−	220(8), 235(6), 353(6), 371(18), 386(6), 401(100), 581(78)	581.2202	581.2175	4.6	
20	28.6	*N*-feruloyloctopamine $C_{18}H_{19}NO_5$	phenolic amine	328/330	133(12), 160(14), 161(71), 175(7), 252(14), 295(16), 310(100), 328(2)	328.1183	328.1185	−0.6	62
21	30.0	N^1,N^4,N^8-tris(dihydrocaffeoyl) spermidine, $C_{34}H_{43}N_3O_9$	phenolic amine	636/638	115(6), 157(8), 186(12), 228(20), 308(80), 350(100), 362(6), 392(20), 472(93), 514(32), 526(12), 636(74)	636.2927	636.2926	0.2	28
22	32.4	α-chaconine, $C_{45}H_{73}NO_{14}$	Glycoalkaloid	896/852	492(1), 558(2), 704(8), 850(100), 896(30)	896.5033	896.5008	2.8	63
23	32.6	α-solanine $C_{45}H_{73}NO_{15}$	Glycoalkaloid	912/868	558(10), 704(100), 720(6), 866(36) 912	912.4988	912.4957	3.4	63
24	33.2	N^1,N^4,N^9,N^{12}-tetra(dihydrocaffeoyl)spermine $C_{46}H_{58}N_4O_{12}$	phenolic amine	857/859	285(15), 365(23), 407(52), 449(36), 529(52), 571(63), 583(9), 613(14), 693(100), 735(40), 857(69)	857.3973	857.3973	0	28
25	34.2	Methylprotodioscin, $C_{51}H_{84}O_{23}$	saponin	1107/−[c]	867(7), 897(5), 1013(8), 1043(19), 1061(100), 1061(MS/MS/MS) − 541(8), 721(8), 867(100), 897(25), 915(8), 1013(38), 1043(50)	1107.5176	1107.5223	−4.3	64
26	34.4	α-chaconine derivative, $C_{48}H_{75}NO_{17}$	Glycoalkaloid	936/938	704(21), 833(14), 850(51), 892(100), 936(11)	936.4940	936.4961	−1.8	
27	34.8	Protodioscin/neoprotodioscin, $C_{51}H_{84}O_{22}$	saponin	1093/1049	431(6), 575(9), 593(9), 737(15), 739(10), 755(73), 883(29), 885(6), 901(100), 902(6), 1047(67)	1093.5417	1093.5431	−1.3	64

J. Agric. Food Chem. 2017, 65, 2258−2274
DOI: 10.1021/acs.jafc.6b05179

Table 2. continued

No.	RT[a] (min)	Compound Name	Structural Class[b]	$[M-H]^-/[M+H]^+$	MS/MS ($[M-H]^-$)	Exact Mass	Calcd Mass	Error (ppm)	Lit. ref
28	35.7	$C_{51}H_{86}O_{21}$+HCOOH	saponin	1079/1035	289(4), 723(10), 725(9), 741(67), 869(21), 887(100), 1033(50), 1079	1079.5643	1079.5638	0.5	
29	36.0	*N*-feruloyltyramine, $C_{18}H_{19}NO_4$	Phenolic acid	312/314	148(36), 178(33), 190(32), 297(27), 312(100)	312.1207	312.1236	−0.9	34
30	39.3	unknown	saponin	946/–	170(9), 203(22), 274(10), 293(5), 333(12), 360(22), 387(17), 404(14), 421(6), 520(7), 546(12), 558(19), 575(100), 577(21), 603(6), 659(6), 737(5), 738(97), 900(6), 946(71)	946.4104			
31	39.5	$C_{43}H_{72}O_{17}$	saponin	929/–	411(4), 507(14), 555(8), 573(10), 719(24), 737(96), 783(12), 883(100), 929(59)	929.4744	929.4746	−0.2	
32	39.9	$C_{43}H_{76}O_{17}$	saponin	933	161(4), 417(2), 513(4), 579(8), 725(100), 741(8), 887(34), 933	933.5054	933.5059	−0.5	
33	40.2	$C_{43}H_{76}O_{16}$	saponin	917/873	113(3), 289(5), 513(7), 543(2), 579(3), 707(2), 725(100), 871(84), 917	917.5103	917.5110	−0.7	
34	41.4	$C_{18}H_{34}O_5$ or $C_{13}H_{34}N_2O_7$		329/331	99(10), 127(15), 139(25), 171(100), 201(11), 211(8), 329(8)	329.2298			
35	41.6	Grossamide $C_{36}H_{36}N_2O_8$		623/625	297(26), 338(11), 430(18), 445(16), 460(100), 501(11), 623.2(45)	623.2415	623.2393	3.5	25,37
36	42.6	$C_{42}H_{44}N_2O_8$		703/705	241(4), 313(8), 315(5), 443(4), 461(5), 587(9), 623(100), 703(28)	703.3012	703.3019	−1.1	

[a]Retention time in minutes. [b]Chemical structures are organized by compound class in Figure 2. [c]$[M+HCOOH]^-$.

Seven compounds listed in Table 2 (***25, 27, 28, 30−33***) were identified as saponin derivatives. This compound class, which contains both hydrophilic sugar and hydrophobic genin moieties, has been found widely in plants. In negative ion mode, the MS spectra of saponins typically produce deprotonated molecular ions $[M-H]^-$ and adduct ions $[M+HCOO]^-$, along with fragment ions indicating the sequential loss of sugar residues. Compound ***25***, with a retention time of 34.2 min and a parent ion at *m/z* 1107 corresponding to the formic acid adduct, yielded daughter ions at *m/z* 1061 $[M-H]^-$ and *m/z* 915 [M−deoxymannose]. Taken together, these ions are characteristic of methylprotodioscin (Figure 2b), which has been reported in fresh and cooked white asparagus (*Asparagus officinalis* L.).[64] Other than the α-chaconine glycoalkaloid found in wound periderms from these four potato cultivars,[36] these saponins are being reported for the first time in potato peel extracts.

Multivariate Analysis of Cultivar-Specific Differences among Polar Metabolites. To provide a comparative interpretation and visualization of the metabolic differences among potato cultivars, the unsupervised Principal Component Analysis (PCA) method for pattern recognition analysis was applied to the LC-MS chromatograms of 28 potato samples from 4 cultivars (7 biological replicates for each cultivar). As shown in Figure 3, a two-dimensional PCA score plot exhibited a clear separation between the Norkotah Russet and Yukon Gold potato cultivars, whereas differences between Atlantic and Chipeta were less distinct. The PCA model with a Pareto-scaled data set[53] was validated by calculating standard parameters for goodness-of-fit and predictability.[65]

Additionally, hierarchical cluster analysis (HCA) was performed using the SIMCA-P+ software to sort the samples or metabolites into groups. A between-group linkage through the cluster method and the squared Euclidean distance as the measurement interval were used to establish the clusters. The dendrogram in Figure 4 was produced by HCA of the potato periderm samples based on the variation of 7 replicates for each cultivar, confirming the results observed with PCA and providing a more detailed view of the relationships between the metabolite profiles of the cultivars. HCA revealed two major clusters, representing the russeted (Norkotah Russet) and white-round potatoes (Atlantic, Chipeta, and Yukon Gold), respectively. The white-round potatoes comprised two subgroups, one consisting of the Yukon Gold cultivar and the second including Atlantic and Chipeta varieties.

Statistical Determination of Polar Metabolites that Discriminate among Potato Cultivars. Orthogonal partial least-squares discriminate analysis (OPLS-DA) was used to identify metabolites present at significantly different relative levels in a russeted cultivar such as Norkotah Russet compared with the white-round potatoes, as well as metabolites that account for differences between Yukon Gold and the remaining cultivars. Unlike PCA, OPLS-DA is a supervised method that evaluates a designated class against others and can reveal the specific metabolites that contribute most significantly to the cultivar distinctions that emerge from PCA and HCA analyses. The significantly different metabolites, or potential biomarkers, were found by using the pq(corr) parameter, i.e., the correlation between p (based on the X component of the OPLS-DA model, which comprises the ions observed by LC-MS for the various metabolites) and q (based on the Y component of the model, which consists of discrete variables specifying the cultivar type).[37] These results are displayed

DOI: 10.1021/acs.jafc.6b05179
J. Agric. Food Chem. 2017, 65, 2258−2274

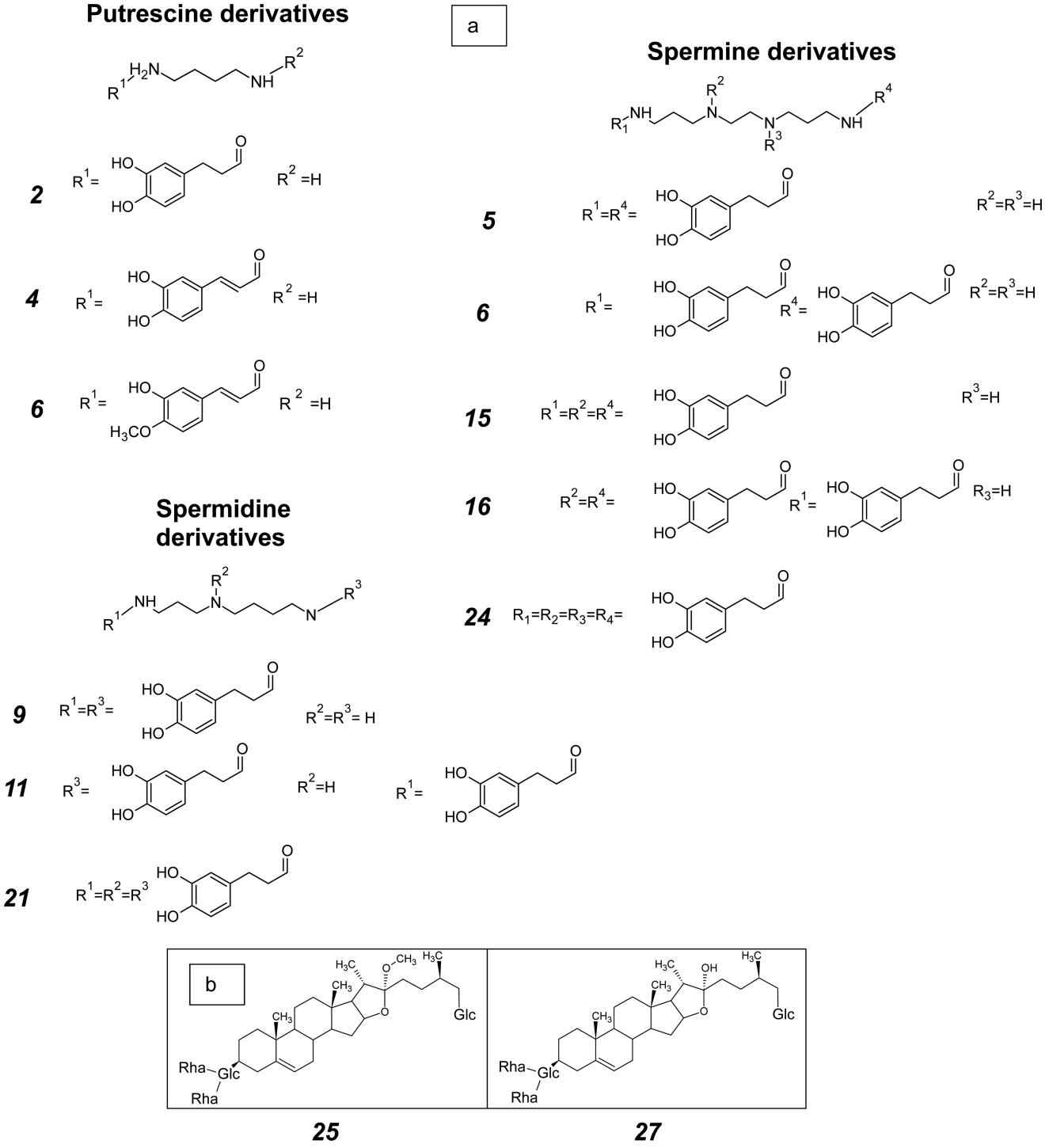

Figure 2. Chemical structures of polar soluble metabolites identified in native potato periderm extracts. (a) polyamines; (b) methylprotodioscin and protodioscin.[64]

graphically in the score plot of Figure S1 and the scatter plot of Figure 5, where metabolites with absolute values of pq(corr) greater than 0.75 were considered to be significant contributors to the differences between native periderms from the four cultivar classes. The statistical validity of the OPLS-DA model was established, *e.g.,* for the russeted Norkotah **R**usset vs the three white-round potatoes by calculating the goodness-of-fit and predictability.[65] Because the four cultivars were grown concurrently in the same location under nominally identical conditions, the anomalous levels of these metabolites may be taken to reflect the genetic and phenotypic differences summarized in Table 1.

Table 3 lists the potential biomarkers of native periderms for the clearly distinct Norkotah Russet and Yukon Gold cultivars, including polar metabolites that are statistically more or less abundant for the particular potato cultivar type. The Norkotah Russet cultivar showed less-abundant glycoalkaloid markers, whereas Yukon Gold displayed a more abundant saponin that is also a putative glycoalkaloid precursor. Polyphenolic amines (spermines, spermidines, putrescines, tyramines) are notably

DOI: 10.1021/acs.jafc.6b05179
J. Agric. Food Chem. 2017, 65, 2258−2274

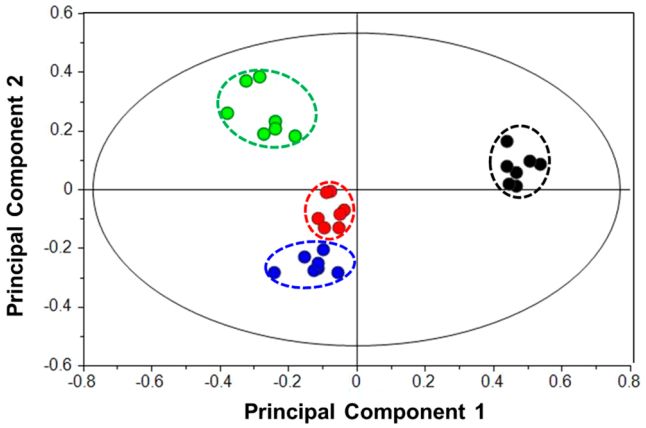

Figure 3. PCA score plot of LC-MS results for seven replicates each of polar native periderm extracts from four native cultivars: Norkotah Russet (black), Atlantic (red), Chipeta (blue), and Yukon Gold (green).

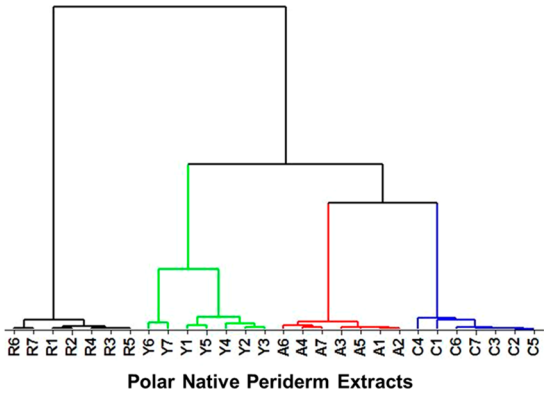

Figure 4. Hierarchical clustering analysis (HCA) dendrogram derived from LC-MS chromatography data sets for polar native periderm extracts from four potato cultivars: Norkotah Russet (black), Atlantic (red), Chipeta (blue), and Yukon Gold (green). The numbers indicate the individual biological replicate samples.

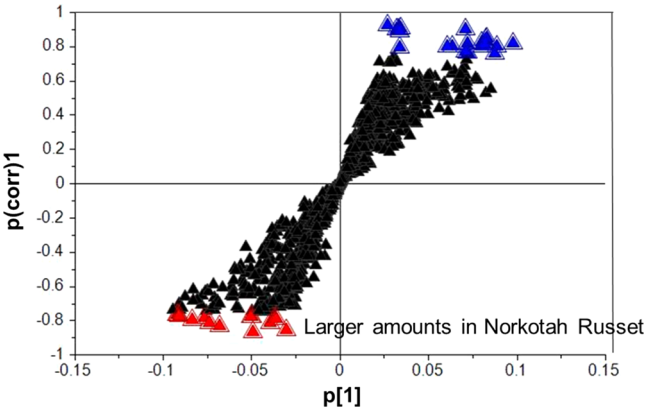

Figure 5. Scatter plot (S-plot) of LC-MS data for polar periderm extracts from Norkotah Russet cultivar vs the three white-round cultivars (Yukon Gold, Atlantic, and Chipeta). The axes p[1] and p(corr)1 correspond to the predictive and orthogonal scores for this scatter plot. The variables denoted in red and blue triangles correspond to metabolites with concentrations that are significantly higher and lower, respectively, in Norkotah Russet as compared to the other three cultivars.

abundant for native Norkotah Russet with the most russeted skin, reinforcing the trends found in day-3 and day-7 wound periderms from these four cultivars,[36] whereas these structures are notably sparse in the least russeted Yukon tissues. Feruloyltyramine and related metabolites, which are markers in both native and wound periderms of the heavily russeted Norkotah Russet cultivar, have also been associated with lesions and with the heavy, cracked skins that are characteristic of scab-infected potato tubers.[25,66] This correlation between russeted phenotype and aromatic amine abundance has also been observed for tubers from two RNAi-silenced potato varieties:[38,41] their skins had notable roughness, brownish color, and russeted scabby lesions, meanwhile showing increased levels of feruloylputrescine and caffeoylputrescine as well as feruloyltyramine−feruloyloctopamine dimers as compared with control tubers.

Given that this compound class has been implicated broadly in plant metabolic signaling[59] and proposed to be involved in protection against potato pathogens,[25,26,66] the current study supports the hypothesis that russeted tubers possess enhanced protective capacities with respect to attack by microbial pathogens. Conversely, wound periderm markers such as feruloylputrescine, coumarylputrescine, N^1,N^4-bis-(dihydrocaffeoyl) spermidine, and N^1,N^4,N^8-tris-(dihydrocaffeoyl) spermidine are found at comparable levels in all four native cultivars, suggesting that any short-term metabolic variations among cultivars could be "smoothed out" as the tuber periderm matures. Phenolic amines such as feruloyltyramine (a marker) and feruloyloctopamine (a non-marker metabolite) have also been implicated by thioacidolysis degradation and by *Streptomyces scabies* infection as constituents of the suberin aromatic domain,[15,25,66] suggesting that these extracted compounds can serve as intermediates in the biosynthesis of the protective biopolyester.

Profiling and Identification of Nonpolar Metabolites. GC-MS metabolite profiling of nonpolar extracts from the native potato periderms revealed 76 MS peaks, demonstrating excellent separation efficiency for aliphatic compounds that include structurally similar homologues. The GC-MS peaks that emerged during the first 16 min were attributable primarily to the pyridine solvent and MSTFA derivatization reagent, as verified by running a blank sample (Figure S2). Overlaid GC-MS chromatograms obtained for 6 biological replicates of each cultivar under identical GC-MS conditions appear in Figure 6, showing a very high degree of reproducibility throughout chromatographic separation of the compounds of interest (17−55 min). Excellent instrumental reproducibility was also demonstrated by duplicate injection of the same samples (data not shown). Although a similar set of ions was detected in each of the native potato periderm samples, the cultivars were distinguished by significant and reproducible differences in the relative MS intensities of those ions.

Fifty of the 76 soluble metabolites in nonpolar extracts from the four cultivars were identified; they are listed in Table 4 by compound class. Overall, these findings demonstrate that, although GC-MS is limited to volatile compounds with molecular weight less than ~800,[30] this analytical method provides useful information for plant metabolomics because of its superlative resolution and the availability of extensive reference compound libraries that facilitate structural elucidation. The extracts contained linear long-chain fatty acids, 1-alkanols, *n*-alkanes, monoacylglycerols, phenolics, sterols, and other compounds, where the first three classes accounted for

DOI: 10.1021/acs.jafc.6b05179
J. Agric. Food Chem. 2017, 65, 2258−2274

Table 3. Metabolites Found at Notably Different Levels in Native Periderm Extracts from Four Potato Cultivars[a]

	Atlantic vs Norkotah Russet, Chipeta, Yukon Gold	**Chipeta** vs Norkotah Russet, Atlantic, Yukon Gold	**Norkotah Russet** vs Atlantic, Chipeta, Yukon Gold	**Yukon Gold** vs Norkotah Russet, Atlantic, Chipeta
POLAR: more abundant			bis(N^1-caffeoyl, N^8-dihydrocaffeoyl) spermidine (***11***)	*m/z* 929, saponin derivative (***31***)[b]
			N-caffeoylputrescine (***4***)[d]	
			N-feruloyltyramine (***29***)[c]	
			N^1,N^4,N^{12}-tris(dihydrocaffeoyl) spermine (***15***)[c]	
POLAR: less abundant			*α*-chaconine (***22***)[e]	*N*-feruloyltyramine (***29***)
			α-solanine (***23***)	N^1,N^4,N^{12}-tris (dihydrocaffeoyl) spermine (***15***)[f]
			Protodioscin/neoprotodioscin (***27***)	*m/z* 936, *α*-chaconine derivative (***26***)
				N-feruloylputrescine (***7***)[d,f]
NONPOLAR: more abundant	*n*-Nonacosane (***74***, C29)		Nonanoic acid (***37***, 9:0); Dodecanoic acid (***38***, 12:0); Pentadecanoic acid (***40***, 15:0)[c]; Tricosanoic acid (***46***, 23:0); Azelaic acid (***54***)[c]	
			Dodecan-1-ol (***58***, C12); Tetradecan-1-ol (***59***, C14); Hexadecan-1-ol (***60***, C16); Octadecan-1-ol (***61***, C18); Eicosan-1-ol (***62***, C20); Docosan-1-ol (***63***, C22); Tetracosan-1-ol (***64***, C24)	
			n-Heneicosane (***70***, C21)[c]	
			4-Hydroxy-3-methoxybenzaldehyde (***78***)	
			4-Hydroxy-3-methoxybenzoic acid (***79***)	
			4-Hydroxybenzoic acid (***80***)	
			Methyl caffeate (***81***)	
			Ferulic acid (***82***)	
			Stigmasterol (***75***)	
			β-Sitosterol (***76***)	
			Unidentified: compounds with retention times of 21.51, 23.91, 24.01, 24.18, 24.99, 27.26, 27.51, 30.51, 30.74, 31.47, 31.81, 34.99, 39.91, 49.52 min	
NONPOLAR: less abundant	Stigmasterol (***75***)	Tetradecanoic acid (***39***, 14:0)[c]	Octacosan-1-ol (***67***, C28); Nonacosan-1-ol (***68***, C29); Triacontan-1-ol (***69***, C30) *n*-Heptacosane (***73***, C27)	Hexacosan-1-ol (***65***, C26)
		Heptadecanoic acid (***42***, 17:0)[c]		*n*-Tricosane (***71***, C23)
		Unidentified: compounds with retention times of 31.37, 31.47, 49.52 min		2-Hydroxydecanedioic acid (***55***)

[a]Metabolites with pq(corr) values greater than 0.75 in OPLS-DA analysis of LC-MS and GC-MS data as shown in Figures 5 and S4. [b]Unidentified potential polar markers are listed according to their *m/z* values and retention times. [c]Also found as a potential marker for wound periderms of the same cultivar.[36,37] [d]Potential marker for wound-healing Atlantic tissues. [e]Potential marker for wound-healing Chipeta tissues. [f]Potential marker for wound-healing Norkotah Russet tissues.

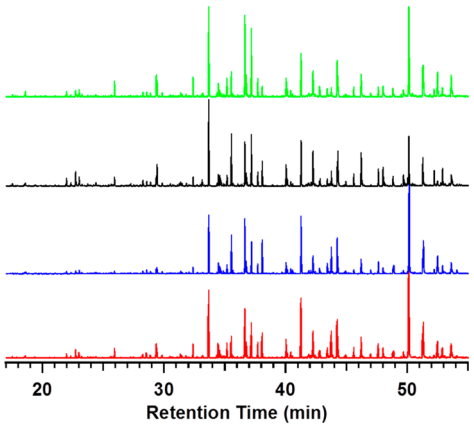

Figure 6. GC-MS chromatograms of nonpolar extracts from native potato periderms, consisting of overlaid data from six replicates for each cultivar: Norkotah Russet (black), Atlantic (red), Chipeta (blue), and Yukon Gold (green). (Peaks from the pyridine solvent and MSTFA derivatization reagent are displayed in Figure S2.)

more than 70% of the recovered soluble materials. The first three classes of compounds have also been found in suberin-associated waxes isolated from potato tuber periderm (by cellulase and pectinase treatment, and then chloroform–methanol extraction);[7] and *Arabidopsis thaliana* roots (by chloroform dipping[67]). Like the root waxes, our nonpolar metabolites (extracted directly from native potato periderms) could be intermediates that undergo desaturation, oxidation, and/or elongation during suberin biosynthesis.[68−70]

The long-chain fatty acids and their derivatives are the most abundant class of nonpolar metabolites extracted from periderm tissues of the four potato cultivars (30–37%). Though the fatty acid chain lengths range from C9 to C30, the C16 and C18 homologues constitute more than half and as much as 15–22% of the total soluble nonpolar constituents for each cultivar. The identified constituents included unsaturated fatty acids such as palmitelaidic (16:1, **50**), linoleic (18:2, **51**), oleic (18:1, **52**), and linolenic (18:3, **53**) analogs, which accounted for 6–9% of the total. Whereas these compounds were not found in suberin-associated waxes,[7,67] they have been reported in potato tuber wound periderm extracts obtained by

DOI: 10.1021/acs.jafc.6b05179
J. Agric. Food Chem. 2017, 65, 2258−2274

Table 4. Metabolites Isolated from Nonpolar Extracts of Four Potato Cultivars

Structural Class and Compound	RT (min)[a]	Atlantic		Chipeta		Norkotah		Yukon Gold	
		%[b]	SD[c]	%[b]	SD[c]	%[b]	SD[c]	%[b]	SD[c]
Saturated fatty acids		**19.69**		**18.02**		**22.19**		**24.21**	
37 Nonanoic acid (9:0)	18.53	0.35	0.01	0.29	0.02	0.49	0.04	0.36	0.04
38 Dodecanoic acid (Lauric, 12:0)	25.66	0.44	0.02	0.36	0.02	0.58	0.05	0.44	0.04
39 Tetradecanoic acid (myristic, 14:0)	29.84	0.57	0.03	0.47	0.03	0.73	0.05	0.64	0.07
40 Pentadecanoic acid (15:0)	31.24	0.27	0.01	0.24	0.02	0.45	0.05	0.26	0.02
41 Hexadecanoic acid (palmitic, 16:0)	33.67	6.34	0.66	5.47	0.86	7.40	0.66	7.84	0.73
42 Heptadecanoic acid (17:0)	34.81	0.31	0.02	0.21	0.01	0.33	0.02	0.28	0.02
43 Octadecanoic acid (stearic, 18:0)	37.17	3.19	0.40	3.01	0.70	4.12	0.52	5.07	1.05
44 Eicosanoic acid (20:0)	40.41	0.81	0.10	0.85	0.06	0.89	0.04	0.89	0.08
45 Docosanoic acid (22:0)	43.42	1.52	0.25	1.76	0.24	1.38	0.17	1.25	0.13
46 Tricosanoic acid (23:0)	44.84	0.49	0.02	0.47	0.02	0.53	0.02	0.44	0.03
47 Hexacosanoic acid (26:0)	48.81	1.02	0.12	1.00	0.09	1.15	0.08	1.11	0.05
48 Octacosanoic acid (28:0)	51.28	2.44	0.41	2.00	0.27	3.04	0.13	3.04	0.25
49 Triacontanoic acid (30:0)	53.61	1.94	0.30	1.90	0.04	1.68	0.21	2.59	0.37
Unsaturated fatty acids		**5.99**		**6.29**		**6.37**		**8.94**	
50 9-Hexadecenoic acid (palmitelaidic, 16:1)	33.19	0.29	0.05	0.25	0.03	0.35	0.05	0.32	0.10
51 9,12-Octadecadienoic acid (linoleic, 18:2)	36.64	3.64	1.01	3.95	1.61	3.88	0.65	5.90	1.80
52 9-Octadecenoic acid (oleic, 18:1)	36.72	1.15	0.25	1.20	0.31	1.08	0.11	1.41	0.32
53 9,12,15-Octadecatrienoic acid (linolenic, 18:3)	36.78	0.91	0.39	0.89	0.30	1.06	0.25	1.32	0.44
Saturated dicarboxylic acids		**4.06**		**4.21**		**2.61**		**1.87**	
54 Azelaic acid	28.89	0.61	0.03	0.56	0.02	0.80	0.06	0.64	0.04
55 2-Hydroxydecanedioic acid	43.76	3.45	0.29	3.65	0.24	1.81	0.16	1.23	0.15
Monoacylglycerols		**1.64**		**1.38**		**2.07**		**1.70**	
56 2,3-Dihydroxypropyl hexadecanoate	42.84	0.61	0.14	0.50	0.05	0.76	0.12	0.63	0.12
57 2,3-Dihydroxypropyl octadecanoate	45.61	1.03	0.27	0.88	0.09	1.31	0.27	1.06	0.25
1-Alkanols		**28.08**		**30.61**		**18.52**		**24.88**	
58 Dodecan-1-ol (C12)	23.73	0.44	0.06	0.35	0.04	0.64	0.07	0.47	0.03
59 Tetradecan-1-ol (C14)	28.11	0.24	0.02	0.19	0.02	0.34	0.03	0.25	0.02
60 Hexadecan-1-ol (C16)	32.04	0.35	0.02	0.35	0.03	0.46	0.02	0.32	0.03
61 Octadecan-1-ol (C18)	35.67	0.58	0.05	0.63	0.05	0.76	0.04	0.57	0.08
62 Eicosan-1-ol (C20)	39.01	0.34	0.02	0.32	0.03	0.46	0.03	0.34	0.03
63 Docosan-1-ol (C22)	42.07	0.95	0.05	0.87	0.05	1.16	0.05	0.94	0.04
64 Tetracosan-1-ol (C24)	44.94	0.66	0.02	0.57	0.04	0.85	0.02	0.58	0.03
65 Hexacosan-1-ol (C26)	47.62	1.93	0.15	1.86	0.22	2.08	0.07	1.33	0.08
66 Heptacosan-1-ol (C27)	48.92	1.15	0.08	1.38	0.17	0.78	0.03	0.71	0.05
67 Octacosan-1-ol (C28)	50.18	13.02	1.26	15.14	1.51	6.85	0.31	11.20	0.83
68 Nonacosan-1-ol (C29)	51.33	5.01	0.33	5.10	0.60	2.07	0.28	4.12	0.55
69 Triacontan-1-ol (C30)	52.51	3.40	0.38	3.85	0.27	2.08	0.18	4.06	0.49
***n*-Alkanes**		**14.17**		**15.36**		**10.95**		**10.89**	
70 *n*-Heneicosane (C21)	34.61	1.08	0.10	1.15	0.13	1.40	0.11	0.90	0.09
71 *n*-Tricosane (C23)	38.07	2.20	0.35	3.21	0.44	2.13	0.26	1.22	0.08
72 *n*-Pentacosane (C25)	41.28	5.86	0.49	6.37	0.44	4.23	0.34	4.27	0.24
73 *n*-Heptacosane (C27)	44.22	4.15	0.30	3.86	0.46	2.47	0.17	3.73	0.28
74 *n*-Nonacosane (C29)	47.01	0.88	0.05	0.77	0.03	0.72	0.04	0.77	0.03
Sterols		**3.42**		**3.33**		**5.61**		**3.71**	
75 Stigmasterol	52.22	0.66	0.05	0.84	0.05	1.87	0.14	1.08	0.07
76 *β*-Sitosterol	52.91	1.67	0.20	1.57	0.14	2.50	0.17	1.57	0.08
77 Cycloartenol	53.71	1.10	0.07	0.92	0.11	1.24	0.14	1.05	0.15
Phenolics		**5.42**		**6.50**		**8.99**		**5.47**	
78 4-Hydroxy-3-methoxybenzaldehyde (vanillin)	23.04	1.19	0.09	0.92	0.11	1.65	0.09	1.20	0.08
79 4-Hydroxybenzoic acid	25.17	0.24	0.02	0.20	0.01	0.33	0.02	0.23	0.02
80 4-Hydroxy-3-methoxybenzoic (vanillic) acid	28.26	0.76	0.04	0.65	0.04	1.05	0.03	0.82	0.06

DOI: 10.1021/acs.jafc.6b05179
J. Agric. Food Chem. 2017, 65, 2258−2274

Table 4. continued

Structural Class and Compound	RT (min)[a]	Atlantic		Chipeta		Norkotah		Yukon Gold	
		%[b]	SD[c]	%[b]	SD[c]	%[b]	SD[c]	%[b]	SD[c]
81 Methyl Caffeate	33.13	0.48	0.03	0.39	0.03	0.91	0.06	0.52	0.04
82 Ferulic acid	34.68	0.59	0.06	0.59	0.04	0.85	0.07	0.61	0.05
83 Caffeic acid	35.53	2.18	0.26	3.75	0.42	4.20	0.58	2.10	0.41
Others		**2.75**		**2.09**		**3.96**		**3.10**	
84 4-Methylbenzoic acid	18.62	0.73	0.03	0.61	0.05	0.95	0.10	0.84	0.11
85 Ethyl 4-ethoxybenzoate	22.81	1.33	0.42	0.98	0.26	2.21	0.50	1.61	0.09
86 Glycerol-3-phosphate	28.56	0.69	0.11	0.51	0.11	0.80	0.06	0.66	0.10
Unidentified (26 unknowns)		**14.78**		**12.21**		**18.73**		**15.19**	
Total		**100**		**100**		**100**		**100**	

[a]Retention time in minutes. [b]Relative mean amounts (w/w percentage of total), calculated by normalizing the integrated area of each peak in the total ion chromatogram with respect to the total area. [c]Standard deviation of six biological replicate samples.

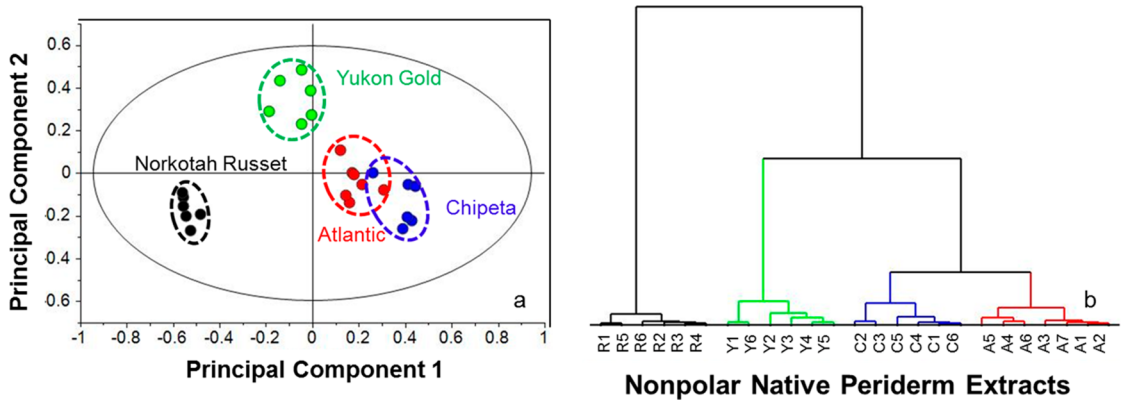

Figure 7. (a) Score plot from PCA analysis of GC-MS data for six replicates each of native periderms from four potato cultivars: Norkotah Russet (black), Atlantic (red), Chipeta (blue), and Yukon Gold (green). (b) Hierarchical clustering analysis (HCA) dendrogram derived from GC-MS chromatography data sets for nonpolar native periderm extracts from four potato cultivars: Norkotah Russet (black), Atlantic (red), Chipeta (blue), and Yukon Gold (green). The numbers indicate the individual biological replicate samples.

similar preparative protocols to ours.[35] Among the unusual constituents is azelaic acid, a saturated C9 diacid reported to prime plants to accumulate salicylic acid, which is in turn a known defense signal for systemic resistance to pathogen infection.[71]

The second most abundant class of soluble monomers is fatty alcohols, amounting to 18−30% of the soluble nonpolar extracts. Fatty alcohols are also reported to be major components in *Arabidopsis* and potato tuber suberin waxes.[7,42,67] Interestingly, very high levels (7−15%) of octacosan-1-ol (C28) were detected in the native potato periderms, consistent with a prior finding in the Desirée variety.[39] Finally, *n*-alkanes comprise the third principal class of monomers (11−15%); as reported in potato wound and native periderms,[37,42,68] it is notable that only odd-numbered long-chain homologues are present.

Multivariate Analysis of Cultivar-Specific Differences among Nonpolar Metabolites. To delineate nonpolar metabolite differences among the native potato periderms, PCA was used to analyze differences in the GC-MS chromatograms of 25 potato samples from the four cultivars (6 biological replicates each). The resulting score plot (Figure 7a) exhibits separation among the four potato cultivars, revealing a striking difference in the first principal component (PC1, 53.4%) for Norkotah Russet and additional distinctions among the cultivars in the second principal component (PC2, 21.4%). As for the corresponding polar extracts described above, Atlantic and Chipeta cultivars displayed similar nonpolar metabolite compositions.

HCA was then used to classify the samples into groups and clarify their relationships, represented by the dendrogram in Figure 7b. This hierarchical clustering showed long vertical lines that indicate more distinct separation between the Norkotah Russet cultivar and the white-round potatoes, confirming the PCA results. The white-round potatoes in turn contained two subgroups, one consisting of Yukon Gold and the second one including the Atlantic and Chipeta cultivars. These last two cultivars were clustered closely by HCA, again confirming the PCA results and showing relationships similar to those found in the polar extracts.

Statistical Determination of Nonpolar Metabolites that Discriminate among Potato Cultivars. Analogously to the polar periderm extracts, OPLS-DA yielded a score plot of the principal nonpolar metabolites responsible for compositional disparities among the potato cultivars that had been indicated by PCA and HCA analyses (Figure S3). These potential biomarkers, which are identified by the retention time and mass at the "wings" of the scatter plot for which the absolute value of pq(corr) exceeds 0.75 (Figure S4), are listed in Table 3. As noted in connection with the polar extracts, the

DOI: 10.1021/acs.jafc.6b05179
J. Agric. Food Chem. 2017, 65, 2258−2274

identical growth conditions of the four cultivars permit interpretation of anomalous metabolite levels in terms of the genetic and phenotypic differences summarized in Table 1.

Whereas the C16 and C18 fatty acids and their derivatives dominated the metabolite pool, they were present at similar levels in all four cultivars. By contrast, a total of 24 identified nonpolar metabolites discriminated between the Norkotah Russet cultivar and the three varieties of white-round potatoes, including 20 more abundant and 4 less-abundant compounds. (The other cultivars together displayed only 9 markers.) The majority of these potential Norkotah Russet biomarkers are soluble aliphatic acids and alcohols with contrasting carbon chain lengths that track their abundance in the extracts: all 13 more-abundant aliphatics have chain lengths ≤24, and all 4 less-abundant aliphatics have lengths ≥27.

Moreover, the proportional representation of these soluble aliphatic markers (Table 4) displays an intriguing pattern. Whereas the 13 more-abundant C9−C24 aliphatics together comprise 9% of the nonpolar metabolites in Norkotah Russet, they represent only 6−7% in the other cultivars, so the observed elevation of Norkotah Russet levels could be expected to have a modest impact on periderm function. In contrast, the 4 less-abundant C26−C30 aliphatic markers together represent much higher relative proportions of the nonpolar metabolite mixtures: 14% in Norkotah Russet and 23−28% in the other three cultivars. The latter long-chain 1-alkanols and *n*-alkanes are precisely the dominant components of suberin-associated waxes that are presumed to regulate water transport and pathogen invasion;[7,42,67,72] the diminished accumulation of such numerically significant nonpolar metabolites has been found to compromise the protective functions of a genetically modified potato periderm[39] and could have an analogous impact on the Norkotah Russet tubers. This hypothesis is also supported by reports of accelerated periderm maturation and thinner wax layers in potatoes exhibiting russeted skin morphology, which have been observed in conjunction with characteristically higher rates of water loss.[73]

Five phenolic compounds were identified as more abundant nonpolar metabolites in Norkotah Russet: ferulic acid, 4-hydroxy-3-methoxybenzaldehyde (vanillin), 4-hydroxy-3-methoxybenzoic acid (vanillic acid), 4-hydroxybenzoic acid, and methyl caffeate. Ferulic acids are thought to form covalent cross-linkages between suberin and cell-wall polysaccharides[74] and are major biosynthetic precursors of vanillin, vanillic acid, and 4-hydroxybenzoic acid. These phenolic compounds also have documented antimicrobial capabilities.[75] The enhanced production of these five phenolic compounds in the Norkotah Russet cultivar could improve the ability of this native periderm to protect tubers against pathogens, compensating for its diminished wax-related waterproofing that can promote microbial invasion. Contributions to the antibacterial defense function in this cultivar could also be made by the abundant phytosterol markers *β*-sitosterol and stigmasterol, which have been implicated in plant innate immunity in *Arabidopsis thaliana*.[76]

Cultivar Comparisons of Suberin Biopolymer Composition in Native Potato Periderms. Solid-state ^{13}C NMR spectra were used to compare the interfacial layers containing suberized cell walls that were isolated from each of the four native potato cultivars. As demonstrated previously in wound periderms from commercial or cultivated potatoes[37,77] and in native periderms including genetically modified tubers,[24] the major structural moieties and their relative proportions can be estimated in plant materials using cross-polarization magic-angle spinning (CPMAS) and either direct-polarization (DPMAS) or multiple-CPMAS methods,[48,78] respectively. The resulting trends can then be coordinated with the multivariate analyses of the corresponding soluble extracts presented above.

Using DPMAS and Multi-CPMAS ^{13}C NMR spectra illustrated in the plots of Figure 8, it was possible first to make compositional distinctions between native and wound periderms. Long-chain methylene groups were sparsely represented in wound tissues regardless of cultivar or healing time point, in accord with their diminished function as barriers to water transpiration. This trend is illustrated quantitatively in Figure 9a, which compares the average ratios of $(CH_2)_n/CH_nO$, $(CH_2)_n$/(aromatic), and $(CH_2)_n$/(carboxyl and amide) for day-7 wound (Wd7) RACY (Norkotah Russet, Atlantic, Chipeta, and Yukon Gold) periderms[37] with native periderms—from the same four cultivars and from a Desirée cultivar described previously.[24] Thus, the relative amounts of $(CH_2)_n$ groups in the suberized wound periderm tissues are small with respect to other major structural moieties.

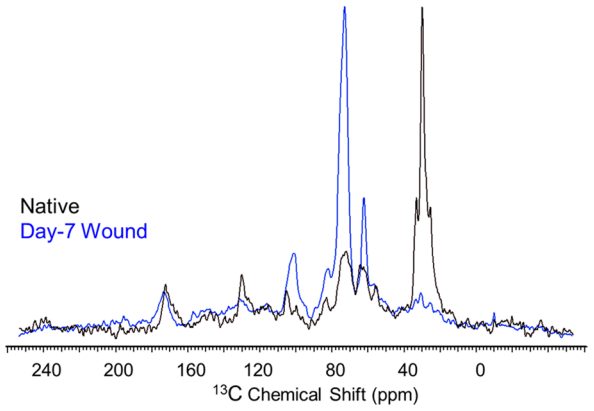

Figure 8. 150 MHz solid-state ^{13}C NMR spectra of suberin-enriched periderm tissues from Chipeta potato tubers, showing the chemical moieties present in the solid interfacial layer and their contrasting proportions estimated by quantitatively reliable methods. Black: native periderms, DPMAS acquisition; blue: day-7 post wounding time point, multi-CPMAS acquisition.[37] Spectra were normalized by matching the heights of the respective carbonyl groups (~170 ppm). The regions used to estimate proportions of the various functional groups are as follows: carboxyl and amide groups (COX, 160−180 ppm), arenes and alkenes ("aromatics," 110−160 ppm), alkoxy groups (46−110 ppm), and alkyl chain methylenes (10−46 ppm).

Second, when the peak ratios were plotted separately for each of the four native cultivars, clear differences were found in the relative amounts of these functional groups. Notably diminished hydrophobic $(CH_2)_n$ content with respect to (CH_nO), aromatic, and carbonyl groups was observed for the most heavily russeted Norkotah Russet cultivar with respect to the least russeted Yukon Gold (Y) cultivar (Figure 9b). Analogous trends have been found for the set of day-7 wound periderms[37] (Figure S5) and the highly permeable *FHT* and *CYP86A33* RNAi-silenced native periderms.[24] These depressed ratios are understandable in light of the significant numbers of abundant polar markers that have phenolic and amide structures, respectively (Table 3). This relative paucity of $(CH_2)_n$ moieties for the native Norkotah Russet solid layer can also be linked to the long-chain less-abundant markers in the

DOI: 10.1021/acs.jafc.6b05179
J. Agric. Food Chem. 2017, 65, 2258−2274

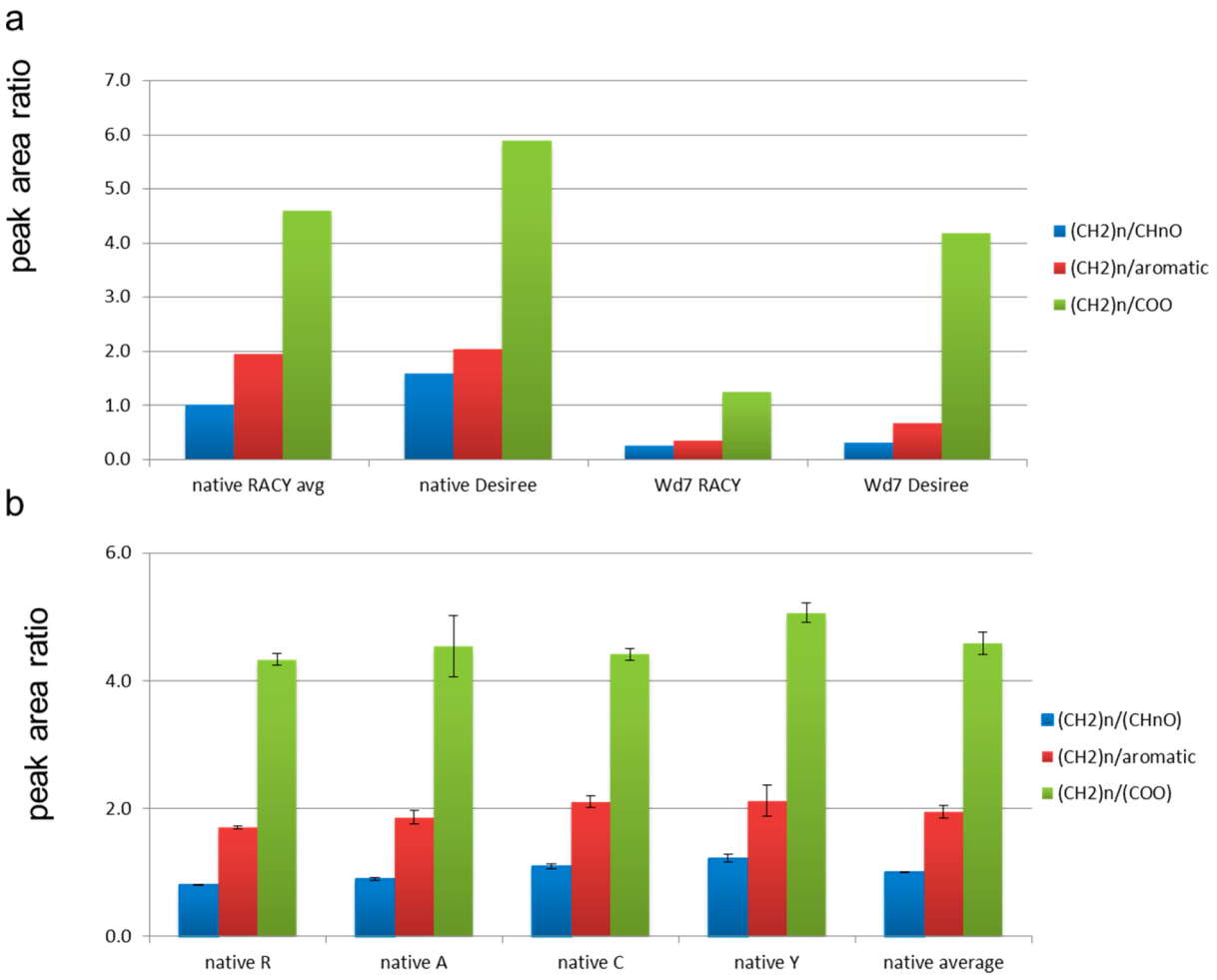

Figure 9. Peak ratios for the solid interfacial layer from suberin-enriched potato periderm samples, showing differences in the proportions of alkyl chain methylenes with respect to other major carbon-containing functional groups. (a) Ratios for day-7 wound-healing tissues[37] vs native periderms, including averages for Norkotah Russet (R), Atlantic (A), Chipeta (C), and Yukon Gold (Y) cultivars as well as a Desirée cultivar.[24] (b) Ratios for native periderms of Norkotah Russet vs Atlantic vs Chipeta vs Yukon Gold cultivars. The regions used to estimate proportions of the various functional groups are as follows: carboxyl and amide groups (COX, 160−180 ppm), arenes and alkenes ("aromatics," 110−160 ppm), alkoxy groups (46−110 ppm), and alkyl chain methylenes (10−46 ppm). The error bars represent the standard error for three different methods of processing.

corresponding nonpolar extract (Table 3), even though the Yukon and Chipeta cultivars also contain similar less-abundant markers. Thus, because the respective less-abundant Norkotah markers constitute 14% of the nonpolar extract, compared with 4% for Yukon and 0.6% for Chipeta, the lowered proportion of $(CH_2)_n$'s in the Norkotah Russet cultivar should dominate the trends observed for the solid-state carbon-containing compositions. In functional terms, the observation of a less hydrophobic periderm for the Norkotah Russet cultivar also aligns with the compromised periderm barrier that is associated with potato russeting.[24,73]

In summary, the molecular entities that contribute to antimicrobial defense and transpirational barrier function in a food staple such as the potato tuber have been identified, by subjecting periderm tissues from four contrasting cultivars to a multisolvent protocol for concurrent extraction of polar and nonpolar soluble metabolites that also yielded an interfacial solid polymer suspension. When coupled with multivariate statistical analysis of LC-MS and GC-MS data for the extracts and quantitative ^{13}C NMR spectra of the solids, this approach yielded a 112-compound metabolic profile and revealed marker compounds that were correlated with differences in the russeting character of the respective potato tuber skins. Particular compound classes, such as phenolic polyamines, phenolic acids, and fatty acids, could be linked to crop marketability factors that are related to the function of the periderm in pathogen resistance, developmental signaling, and waterproofing.

For instance, the heavily russeted Norkotah Russet cultivar exhibited elevated levels of antimicrobial polyphenolic amines but diminished accumulation of long-chain fatty acids and alcohols that may be essential to avoid tissue desiccation. In addition to acting as defensive agents and growth modulators, the metabolites and potential biomarkers can be viewed as likely intermediates in suberin biosynthesis if they are observed among the depolymerization products of potato periderm tissues.[9,12,13,15,17] The solid aromatic−aliphatic suberin polyester within the periderm of this cultivar also showed a relative deficiency in long-chain $(CH_2)_n$ groups that we attribute to less-vigorous polymerization of the soluble metabolites and a concomitantly compromised transpirational barrier.

Despite the observation of analogous compositional cultivar-specific variations among the solid native and wound periderm tissues, native suberins from all four cultivars were found to be notably richer in $(CH_2)_n$ groups than any of the wound periderms. Taken together, these findings provide comprehen-

DOI: 10.1021/acs.jafc.6b05179
J. Agric. Food Chem. 2017, 65, 2258−2274

sive molecular insights with the potential to guide the development of potato cultivars that resist both pathogenic attack and water loss during growth and postharvest processing, improving their practical suitability for end use as food products.

■ ASSOCIATED CONTENT

Supporting Information

The Supporting Information is available free of charge on the ACS Publications website at DOI: 10.1021/acs.jafc.6b05179.

Figure S1: OPLS-DA score plot of LC-MS data from polar potato periderm extracts. Figure S2: GC-MS chromatograms of nonpolar extracts. Figure S3: OPLS-DA score plot of GC-MS data from nonpolar extracts. Figure S4: S-plot of OPLS-DA analysis for nonpolar extracts. Figure S5: Peak ratios for the solid interfacial layer from suberin-enriched wound tissues (PDF)

■ AUTHOR INFORMATION

Corresponding Author

*Tel: +1 212-650-8916. E-mail: rstark@ccny.cuny.edu.

ORCID

Ruth E. Stark: 0000-0002-3132-4580

Funding

This research was supported with funding from the U.S. National Science Foundation (NSF) (MCB-0843627 and 1411984 to R.E.S.) and a mobility grant from the Spanish Ministry of Education (JC2010-0147 to O.S.). The NMR resources were supported by The City College of New York (CCNY) and the CUNY Institute for Macromolecular Assemblies, with infrastructural assistance provided by the National Institutes of Health through the National Institute on Minority Health and Health Disparities (5G12MD007603-30). The TOF-MS and GC-MS instruments were provided through NSF grants CHE-0520963 and CHE-0840498, respectively.

Notes

The authors declare no competing financial interest.

■ ACKNOWLEDGMENTS

We gratefully acknowledge Joe Nuñez from the University of California at Davis for providing the fresh potato cultivars, Cristina Veresmortean for technical support of the GC-MS instrument, and Nancy Medina for method development during the early stages of this project.

■ REFERENCES

(1) Evert, R. F. *Esau's Plant Anatomy:Meristems, Cells, and Tissues of the Plant Body: Their Structure, Function, and Development*; JohnWiley & Sons: Hoboken, NJ, 2006.

(2) Lulai, E. C. Tuber Quality. In *Potato Biology and Biotechnology: Advances and Perspectives*; Elsevier B.V.: Amsterdam, 2007.

(3) Schieber, A.; Aranda Saldana, M. D. Potato Peels: A Source of Nutritionally and Pharmacologically Interesting Compounds − A Review. *Food* **2009**, *3*, 23−29.

(4) Rodriguez de Sotillo, D.; Hadley, M.; Wolf-Hall, C. Potato Peel Extract a Nonmutagenic Antioxidant with Potential Antimicrobial Activity. *J. Food Sci.* **1998**, *63* (5), 907−910.

(5) Garcia, H.; Ferreira, R.; Martins, C.; Sousa, A. F.; Freire, C. S. R.; Silvestre, A. J. D.; Kunz, W.; Rebelo, L. P. N.; Silva Pereira, C. Ex situ reconstitution of the plant biopolyester suberin as a film. *Biomacromolecules* **2014**, *15* (5), 1806−1813.

(6) Tamm, I.; Heinämäki, J.; Laidmäe, I.; Rammo, L.; Paaver, U.; Ingebrigtsen, S. G.; Škalko-Basnet, N.; Halenius, A.; Yliruusi, J.; Pitkänen, P.; et al. Development of Suberin Fatty Acids and Chloramphenicol-Loaded Antimicrobial Electrospun Nanofibrous Mats Intended for Wound Therapy. *J. Pharm. Sci.* **2016**, *105* (3), 1239−1247.

(7) Schreiber, L.; Franke, R.; Hartmann, K. Wax and suberin development of native and wound periderm of potato (Solanum tuberosum L.) and its relation to peridermal transpiration. *Planta* **2005**, *220* (4), 520−530.

(8) Holloway, P. J. Some variations in the composition of suberin from the cork layers of higher plants. *Phytochemistry* **1983**, *22*, 495−502.

(9) Graça, J.; Santos, S. Suberin: the biopolyester of plants' skin. *Macromol. Biosci.* **2007**, *7* (2), 128−135.

(10) Company-Arumi, D.; Figueras, M.; Salvado, V.; Molinas, M.; Serra, O.; Antico, E. The Identification and Quantification of Suberin Monomers of Root and Tuber Periderm from Potato (Solanum tuberosum) as Fatty Acyl tert-Butyldimethylsilyl Derivatives. *Phytochem. Anal.* **2016**, *27* (6), 326−335.

(11) Graça, J.; Pereira, H. Suberin structure in potato periderm: glycerol, long-chain monomers, and glyceryl and feruloyl dimers. *J. Agric. Food Chem.* **2000**, *48*, 5476−5483.

(12) Graça, J.; Cabral, V.; Santos, S.; Lamosa, P.; Serra, O.; Molinas, M.; Schreiber, L.; Kauder, F.; Franke, R. Partial depolymerization of genetically modified potato tuber periderm reveals intermolecular linkages in suberin polyester. *Phytochemistry* **2015**, *117*, 209−219.

(13) Wang, W.; Tian, S.; Stark, R. E. Isolation and identification of triglycerides and ester oligomers from partial degradation of potato suberin. *J. Agric. Food Chem.* **2010**, *58* (2), 1040−1045.

(14) Lapierre, C.; Pollet, B.; Negrel, J. N. The phenolic domain of potato suberin: structural comparison with lignins. *Phytochemistry* **1996**, *42* (4), 949−953.

(15) Negrel, J.; Pollet, B.; Lapierre, C. Ether-linked ferulic acid amides in natural and wound periderms of potato tuber. *Phytochemistry* **1996**, *43* (6), 1195−1199.

(16) Marques, A.; Pereira, H.; Meier, D.; Faix, O. Structural Characterization of Cork Lignin by Thioacidolysis and Permanganate Oxidation. *Holzforschung* **1999**, *53* (2), 167−174.

(17) Bernards, M. A. Demystifying suberin. *Can. J. Bot.* **2002**, *80*, 227−240.

(18) Garbow, J. R.; Ferrantello, L. M.; Stark, R. E. 13C nuclear magnetic resonance study of suberized potato cell wall. *Plant Physiol.* **1989**, *90*, 783−787.

(19) Stark, R. E.; Garbow, J. R. Nuclear magnetic resonance relaxation studies of plant polyester dynamics. 2. suberized potato cell wall. *Macromolecules* **1992**, *25*, 149−154.

(20) Lopez, M. L.; Bernards, M. A.; Zajicek, J.; Lewis, N. G. Hydroxycinnamic acid-derived polymers constitute the polyaromatic domain of suberin. *J. Biol. Chem.* **1995**, *270*, 7382−7386.

(21) Moire, L.; Schmutz, A.; Buchala, A.; Yan, B.; Stark, R. E.; Ryser, U. Glycerol is a suberin monomer. New experimental evidence for an old hypothesis. *Plant Physiol.* **1999**, *119*, 1137−1146.

(22) Yan, B.; Stark, R. E. Biosynthesis, Molecular Structure, and Domain Architecture of Potato Suberin: A 13 C NMR Study Using Isotopically Labeled Precursors. *J. Agric. Food Chem.* **2000**, *48* (8), 3298−3304.

(23) Mattinen, M.-L.; Filpponen, I.; Järvinen, R.; Li, B.; Kallio, H.; Lehtinen, P.; Argyropoulos, D. Structure of the polyphenolic component of suberin isolated from potato (Solanum tuberosum var. Nikola). *J. Agric. Food Chem.* **2009**, *57* (20), 9747−9753.

(24) Serra, O.; Chatterjee, S.; Figueras, M.; Molinas, M.; Stark, R. E. Deconstructing a plant macromolecular assembly: chemical architecture, molecular flexibility, and mechanical performance of natural and engineered potato suberins. *Biomacromolecules* **2014**, *15*, 799−811.

(25) King, R. R.; Calhoun, L. A. Characterization of cross-linked hydroxycinnamic acid amides isolated from potato common scab lesions. *Phytochemistry* **2005**, *66* (20), 2468−2473.

(26) Back, K. Hydroxycinnamic acid amides and their possible utilization for enhancing agronomic traits. *Plant Pathol. J.* **2001**, *17* (3), 123−127.

DOI: 10.1021/acs.jafc.6b05179
J. Agric. Food Chem. 2017, 65, 2258−2274

(27) Savarese, S.; Andolfi, A.; Cimmino, A.; Carputo, D.; Frusciante, L.; Evidente, A. Glycoalkaloids as biomarkers for recognition of cultivated, wild, and somatic hybrids of potato. *Chem. Biodiversity* **2009**, *6* (4), 437−446.
(28) Shakya, R.; Navarre, D. A. Rapid screening of ascorbic acid, glycoalkaloids, and phenolics in potato using high-performance liquid chromatography. *J. Agric. Food Chem.* **2006**, *54* (15), 5253−5260.
(29) Kim, H. K.; Choi, Y. H.; Verpoorte, R. NMR-based metabolomic analysis of plants. *Nat. Protoc.* **2010**, *5* (3), 536−549.
(30) Weckwerth, W. *Metabolomics - Methods and Protocols*; Humana Press: Totowa, NJ, 2007.
(31) Parr, A. J.; Mellon, F. A.; Colquhoun, I. J.; Davies, H. V. Dihydrocaffeoyl polyamines (kukoamine and allies) in potato (Solanum tuberosum) tubers detected during metabolite profiling. *J. Agric. Food Chem.* **2005**, *53* (13), 5461−5466.
(32) Shakya, R.; Navarre, D. A. LC-MS analysis of solanidane glycoalkaloid diversity among tubers of four wild potato species and three cultivars (Solanum tuberosum). *J. Agric. Food Chem.* **2008**, *56* (16), 6949−6958.
(33) Ieri, F.; Innocenti, M.; Andrenelli, L.; Vecchio, V.; Mulinacci, N. Rapid HPLC/DAD/MS method to determine phenolic acids, glycoalkaloids and anthocyanins in pigmented potatoes (Solanum tuberosum L.) and correlations with variety and geographical origin. *Food Chem.* **2011**, *125* (2), 750−759.
(34) Narváez-Cuenca, C.-E.; Vincken, J.-P. P.; Zheng, C.; Gruppen, H. Diversity of (dihydro) hydroxycinnamic acid conjugates in Colombian potato tubers. *Food Chem.* **2013**, *139* (1−4), 1087−1097.
(35) Yang, W.-L.; Bernards, M. A. Metabolite profiling of potato (Solanum tuberosum L.) tubers during wound-induced suberization. *Metabolomics* **2007**, *3*, 147−159.
(36) Dastmalchi, K.; Cai, Q.; Zhou, K.; Huang, W.; Serra, O.; Stark, R. E. Completing the jigsaw puzzle of wound-healing potato cultivars: metabolite profiling and antioxidant activity of polar extracts. *J. Agric. Food Chem.* **2014**, *62*, 7963−7975.
(37) Dastmalchi, K.; Kallash, L.; Wang, I.; Phan, V. C.; Huang, W.; Serra, O.; Stark, R. E. Defensive Armor of Potato Tubers: Nonpolar Metabolite Profiling, Antioxidant Assessment, and Solid-State NMR Compositional Analysis of Suberin-Enriched Wound-Healing Tissues. *J. Agric. Food Chem.* **2015**, *63* (30), 6810−6822.
(38) Serra, O.; Hohn, C.; Franke, R.; Prat, S.; Molinas, M.; Figueras, M. A feruloyl transferase involved in the biosynthesis of suberin and suberin-associated wax is required for maturation and sealing properties of potato periderm. *Plant J.* **2010**, *62* (2), 277−290.
(39) Serra, O.; Soler, M.; Hohn, C.; Franke, R.; Schreiber, L.; Prat, S.; Molinas, M.; Figueras, M. Silencing of StKCS6 in potato periderm leads to reduced chain lengths of suberin and wax compounds and increased peridermal transpiration. *J. Exp. Bot.* **2009**, *60* (2), 697−707.
(40) Serra, O.; Soler, M.; Hohn, C.; Sauveplane, V.; Pinot, F.; Franke, R.; Schreiber, L.; Prat, S.; Molinas, M.; Figueras, M. CYP86A33-targeted gene silencing in potato tuber alters suberin composition, distorts suberin lamellae, and impairs the periderm's water barrier function. *Plant Physiol.* **2009**, *149* (2), 1050−1060.
(41) Landgraf, R.; Smolka, U.; Altmann, S.; Eschen-Lippold, L.; Senning, M.; Sonnewald, S.; Weigel, B.; Frolova, N.; Strehmel, N.; Hause, G.; et al. The ABC transporter ABCG1 is required for suberin formation in potato tuber periderm. *Plant Cell* **2014**, *26* (8), 3403−3415.
(42) Verdaguer, R.; Soler, M.; Serra, O.; Garrote, A.; Fernández, S.; Company-Arumí, D.; Anticó, E.; Molinas, M.; Figueras, M. Silencing of the potato StNAC103 gene enhances the accumulation of suberin polyester and associated wax in tuber skin. *J. Exp. Bot.* **2016**, *67*, 5415−5427.
(43) Ginzberg, I.; Minz, D.; Faingold, I.; Soriano, S.; Mints, M.; Fogelman, E.; Warshavsky, S.; Zig, U.; Yermiyahu, U. Calcium Mitigated Potato Skin Physiological Disorder. *Am. J. Potato Res.* **2012**, *89* (5), 351−362.
(44) Sabba, R. P.; Lulai, E. C. Histological Analysis of the Maturation of Native and Wound Periderm in Potato (Solanum tuberosum L.) Tuber. *Ann. Bot.* **2002**, *90* (1), 1−10.
(45) Pacchiano, R. A.; Sohn, W.; Chlanda, V. L.; Garbow, J. R.; Stark, R. E. Isolation and spectral characterization of plant cuticle polyesters. *J. Agric. Food Chem.* **1993**, *41*, 78−83.
(46) Navarre, D. A.; Pillai, S. S.; Shakya, R.; Holden, M. J. HPLC profiling of phenolics in diverse potato genotypes. *Food Chem.* **2011**, *127* (1), 34−41.
(47) Fung, B. M.; Khitrin, A. K.; Ermolaev, K. An improved broadband decoupling sequence for liquid crystals and solids. *J. Magn. Reson.* **2000**, *142* (1), 97−101.
(48) Johnson, R. L.; Schmidt-Rohr, K. Quantitative Solid-State 13C NMR with Signal Enhancement by Multiple Cross Polarization. *J. Magn. Reson.* **2013**, *239*, 44−49.
(49) Morcombe, C. R.; Zilm, K. W. Chemical shift referencing in MAS solid state NMR. *J. Magn. Reson.* **2003**, *162* (2), 479−486.
(50) Chatterjee, S.; Prados-Rosales, R.; Itin, B.; Casadevall, A.; Stark, R. E. Solid-state NMR Reveals the Carbon-based Molecular Architecture of Cryptococcus neoformans Fungal Eumelanins in the Cell Wall. *J. Biol. Chem.* **2015**, *290* (22), 13779−13790.
(51) Katajamaa, M.; Miettinen, J.; Oresic, M. MZmine: toolbox for processing and visualization of mass spectrometry based molecular profile data. *Bioinformatics* **2006**, *22* (5), 634−636.
(52) Pluskal, T.; Castillo, S.; Villar-Briones, A.; Oresic, M. MZmine 2: modular framework for processing, visualizing, and analyzing mass spectrometry-based molecular profile data. *BMC Bioinf.* **2010**, *11*, 395.
(53) Eriksson, L.; Johansson, E.; Kettaneh-Wold, N.; Trygg, J.; Wikstrom, C.; Word, S. *Multi- and Megavariate Data Analysis, Basic Principles and Applications*, 2nd ed.; Umetric Academy: Umea, 2006.
(54) Prasad Maharjan, R.; Ferenci, T. Global metabolite analysis: The influence of extraction methodology on metabolome profiles of Escherichia coli. *Anal. Biochem.* **2003**, *313* (1), 145−154.
(55) Mushtaq, M. Y.; Choi, Y. H.; Verpoorte, R.; Wilson, E. G. Extraction for metabolomics: access to the metabolome. *Phytochem. Anal.* **2014**, *25* (4), 291−306.
(56) Dettmer, K.; Nürnberger, N.; Kaspar, H.; Gruber, M. A.; Almstetter, M. F.; Oefner, P. J. Metabolite extraction from adherently growing mammalian cells for metabolomics studies: optimization of harvesting and extraction protocols. *Anal. Bioanal. Chem.* **2011**, *399* (3), 1127−1139.
(57) Bouchereau, A.; Aziz, A.; Larher, F.; Martin-Tanguy, J. Polyamines and environmental challenges: recent development. *Plant Sci.* **1999**, *140* (2), 103−125.
(58) Shen, W.; Nada, K.; Tachibana, S. Involvement of polyamines in the chilling tolerance of cucumber cultivars. *Plant Physiol.* **2000**, *124* (1), 431−439.
(59) Walden, R.; Cordeiro, A.; Tiburcio, A. F. Polyamines: small molecules triggering pathways in plant growth and development. *Plant Physiol.* **1997**, *113* (4), 1009−1013.
(60) Matsuda, F.; Morino, N.; Ano, R.; Kuzawa, M.; Wakasa, K.; Miyagawa, H. Metabolic flux analysis of the phenylpropanoid pathway in elicitor-treated potato tuber tissue. *Plant Cell Physiol.* **2005**, *46* (3), 454−466.
(61) Clifford, M. N.; Johnston, K. L.; Knight, S.; Kuhnert, N. Hierarchical Scheme for LC-MSn Identification of Chlorogenic Acids. *J. Agric. Food Chem.* **2003**, *51* (1), 2900−2911.
(62) Narváez-Cuenca, C.-E.; Vincken, J.-P.; Gruppen, H. Identification and quantification of (dihydro) hydroxycinnamic acids and their conjugates in potato by UHPLC−DAD−ESI-MSn. *Food Chem.* **2012**, *130* (3), 730−738.
(63) Distl, M.; Wink, M. Identification and Quantification of Steroidal Alkaloids from Wild Tuber-Bearing Solanum Species by HPLC and LC-ESI-MS. *Potato Res.* **2009**, *52* (1), 79−104.
(64) Dawid, C.; Hofmann, T. Quantitation and bitter taste contribution of saponins in fresh and cooked white asparagus (Asparagus officinalis L.). *Food Chem.* **2014**, *145*, 427−436.
(65) Worley, B.; Powers, R. Multivariate Analysis in Metabolomics. *Curr. Metabolomics* **2013**, *1*, 92−107.
(66) King, R. R.; Calhoun, L. A. A feruloyltyramine trimer isolated from potato common scab lesions. *Phytochemistry* **2010**, *71* (17−18), 2187−2189.

DOI: 10.1021/acs.jafc.6b05179
J. Agric. Food Chem. 2017, 65, 2258−2274

(67) Kosma, D. K.; Molina, I.; Ohlrogge, J. B.; Pollard, M. Identification of an Arabidopsis fatty alcohol:caffeoyl-Coenzyme A acyltransferase required for the synthesis of alkyl hydroxycinnamates in root waxes. *Plant Physiol.* **2012**, *160* (1), 237−248.
(68) Yang, W.-L.; Bernards, M. A. Wound-induced metabolism in potato (Solanum tuberosum) tubers. *Plant Signaling Behav.* **2006**, *1*, 59−66.
(69) Li, Y.; Beisson, F.; Koo, A. J. K.; Molina, I.; Pollard, M.; Ohlrogge, J. Identification of acyltransferases required for cutin biosynthesis and production of cutin with suberin-like monomers. *Proc. Natl. Acad. Sci. U. S. A.* **2007**, *104* (46), 18339−18344.
(70) Pollard, M.; Beisson, F.; Li, Y.; Ohlrogge, J. B. Building lipid barriers: biosynthesis of cutin and suberin. *Trends Plant Sci.* **2008**, *13* (5), 236−246.
(71) Jung, H. W.; Tschaplinski, T. J.; Wang, L.; Glazebrook, J.; Greenberg, J. T. Priming in systemic plant immunity. *Science* **2009**, *324* (5923), 89−91.
(72) Li, Y.; Beisson, F.; Ohlrogge, J.; Pollard, M. Monoacylglycerols are components of root waxes and can be produced in the aerial cuticle by ectopic expression of a suberin-associated acyltransferase. *Plant Physiol.* **2007**, *144* (3), 1267−1277.
(73) Lulai, E. C.; Orr, P. H. Techniques for detecting and measuring developmental and maturational changes in tuber native periderm. *Am. Potato J.* **1994**, *71* (8), 489−505.
(74) Riley, R. G.; Kolattukudy, P. E. Evidence for covalently attached p-coumaric acid and ferulic acid in cutins and suberins. *Plant Physiol.* **1975**, *56* (5), 650−654.
(75) Akyol, H.; Riciputi, Y.; Capanoglu, E.; Caboni, M.; Verardo, V. Phenolic Compounds in the Potato and Its Byproducts: An Overview. *Int. J. Mol. Sci.* **2016**, *17* (6), 835.
(76) Wang, K.; Senthil-Kumar, M.; Ryu, C.-M.; Kang, L.; Mysore, K. S. Phytosterols Play a Key Role in Plant Innate Immunity against Bacterial Pathogens by Regulating Nutrient Efflux into the Apoplast. *Plant Physiol.* **2012**, *158* (4), 1789−1802.
(77) Stark, R. E.; Yan, B.; Ray, A. K.; Chen, Z.; Fang, X.; Garbow, J. R. NMR studies of structure and dynamics in fruit cuticle polyesters. *Solid State Nucl. Magn. Reson.* **2000**, *16* (1−2), 37−45.
(78) Serra, O.; Chatterjee, S.; Huang, W.; Stark, R. E. Mini-review: what nuclear magnetic resonance can tell us about protective tissues. *Plant Sci.* **2012**, *195*, 120−124.
(79) Fang, N.; Yu, S.; Prior, R. L. LC/MS/MS characterization of phenolic constituents in dried plums. *J. Agric. Food Chem.* **2002**, *50* (12), 3579−3585.
(80) Wu, S. B.; Meyer, R. S.; Whitaker, B. D.; Litt, A.; Kennelly, E. J. A new liquid chromatography-mass spectrometry-based strategy to integrate chemistry, morphology, and evolution of eggplant (Solanum) species. *J. Chromatogr. A* **2013**, *1314*, 154−172.

DOI: 10.1021/acs.jafc.6b05179
J. Agric. Food Chem. 2017, 65, 2258−2274